

**ONTOGENY AND CRANIAL MORPHOLOGY OF THE BASAL  
CARNIVOROUS DINOCEPHALIAN, *ANTEOSAURUS MAGNIFICUS*  
FROM THE *TAPINOCEPHALUS* ASSEMBLAGE ZONE OF THE SOUTH  
AFRICAN KAROO**

Ashley Kruger

A Dissertation submitted to the Faculty of Science, University of the  
Witwatersrand, Johannesburg, in fulfilment of the requirements for the degree of  
Master of Science.

Johannesburg, 2014

*The financial assistance of the National Research Foundation (NRF) towards this  
research is hereby acknowledged. Opinions expressed and conclusions arrived at,  
are those of the author and are not necessarily to be attributed to the NRF.*

## **DECLARATION**

I declare that this dissertation is my own, unaided work. It is being submitted for the Degree of Master of Science at the University of the Witwatersrand, Johannesburg, South Africa. It has not been submitted before for any degree or examination at any other university.

A handwritten signature in black ink, appearing to be 'J. S. S. S.', written over a horizontal line.

On this 25 day of April 2014 in Johannesburg

## ABSTRACT

Anteosaurus (Therapsida: Dinocephalia: Anteosauria) were the dominant terrestrial predators during the late Middle Permian period and became extinct at the close of the *Tapinocephalus* Assemblage Zone. Only two genera of anteosaurus, *Australosyodon* and *Anteosaurus*, are recognised from the Karoo rocks of South Africa. A newly discovered small anteosaurid skull from the Abrahamskraal Formation is fully described. Because of its relatively large orbits, the unfused nature of its sutures, and the lack of replacement teeth in the dental alveoli, the specimen is considered to be a juvenile *Anteosaurus magnificus*. A full computer-aided 3-D reconstruction of the skull enabled cranial measurements to be taken for an allometric analysis which included twenty-three measurements and eleven specimens. Positive allometry was found for four of the measurements suggesting fast growing in the temporal region, and a significant difference in the development of the postorbital bar and suborbital bar between juveniles and adults. Phylogenetic research shows that the Russian anteosaurids to be forerunners to *Anteosaurus*, and because the juvenile *Anteosaurus* (BP/1/7074) manifests many features of both *Syodon* and *Titanophoneus*, it is suggested that ontogenetic growth of *Anteosaurus* follows Haeckel's Law.

## **ACKNOWLEDGEMENTS**

I am indebted to my supervisors Prof. B. S. Rubidge and Dr. F. Abdala for their support and guidance during this dissertation, and for always keeping an open door for me to ask anything, at any time.

Thanks to Mrs. C. Kemp of the Evolutionary Studies Institute for the outstanding preparation of the specimen described in this dissertation and enthusiasm for this project.

Financial support was received from the National Research Foundation (NRF) through a linked bursary under Prof. B.S. Rubidge. Additional funds were received from the Palaeontological Scientific Trust (PAST).

Thanks to Drs. F. Abdala and J. Choiniere for guidance pertaining to the preparation of illustrations presented in this dissertation, as well as direction with the allometric analysis. Thanks to Drs. K. Carlson and T. Jashashvili for Micro C-T scanning of the specimen and Dr. T. Jashashvili for training on the Avizo software package.

Special thanks to E. Odes for providing me with a working computer in desperate times, and for all the long chats over coffee and lunches at the PIG, shared about palaeontology, life and everything else. You are truly a great friend.

I would like to thank my mother, Mrs. L. Kruger and family, especially Ms. J. Capon for their support in my pursuit to follow my dreams and further my studies in this field as well as for financial support over the years.

Finally I would like to thank my girlfriend N. Barbolini for all her support over the duration of this dissertation, always pushing me to be my best, and never giving up on me. Without her this dissertation would not be a reality.

In memory of my Grandparents

Beryl Capon

(23 November 1928 – 15 October 1999)

and

David Capon

(11 December 1926 – 27 April 2009)

## **TABLE OF CONTENTS**

### **CHAPTER ONE: INTRODUCTION AND LITERATURE REVIEW**

1.1 General Introduction	1
1.2 Historic Review of the Anteosauridae	2
1.2.1 Anteosaurids from South Africa	6
1.2.2 Anteosaurids from Russia	8
1.2.3 Anteosaurids from Brazil	12
1.2.4 Anteosaurids from China	13
1.3 Dentition and Tooth Replacement	14

### **CHAPTER TWO: MATERIALS AND METHODOLOGY**

2.1 Specimens	17
2.2 Preparation	18
2.3 Microfocus X-Ray Computed Tomography (CT) Scanning and Segmentation	19
2.4 3-D Reconstruction	21
2.5 Tooth Replacement	22
2.6 Allometric Analysis	22

## **CHAPTER THREE: RESULTS**

3.1 Systematic Palaeontology	25
3.2 Description	
3.2.1 General Comments	27
3.2.2 Skull Roof	29
3.2.3 Palate	43
3.2.4 Occiput	48
3.2.5 Lower Jaw	52
3.2.6 Dentition	54
3.2.7 Cervical Vertebrae	55
3.3 Microfocus X-Ray Computer Tomography (CT) Scanning and 3-D Reconstruction	61
3.4 Tooth Replacement	67
3.5 Allometry	72

## **CHAPTER FOUR: DISCUSSION AND CONCLUSION**

4.1 Growth Model of <i>Anteosaurus magnificus</i>	76
4.2 Heterochronic Process in Anteosauria	78
4.3 Conclusion	83

<b>5 REFERENCES</b>	<b>85</b>
---------------------	-----------



## **6 APPENDICES**

- 6.1: Appendix A: List of measurements taken for allometric analysis 97
- 6.2: Appendix B: Table of distances (in mm) of the different  
measurements presented in Appendix A for the ten  
most completely preserved skulls of *Anteosaurus magnificus*. 99

## LIST OF FIGURES

Figure 1.1:	Cladogram showing the phylogenetic relationships of the main dinocephalian groups (King, 1988).	3
Figure 1.2:	Cladogram of anteosaurian relationships (Kammerer, 2011). <i>Doliosauriscus yanshinovi</i> is regarded as a junior synonym for <i>Titanophoneus potens</i> .	4
Figure 2.1:	Illustration of the skull of <i>Anteosaurus</i> showing the measurements used in the allometric analysis. (A) dorsal view; (B) ventral view; and (C) lateral view. (B) Redrawn after Boonstra (1969).	24
Figure 3.1:	Photograph (A) and illustration (B) of BP/1/7074 in lateral view. Scale bars equal 1cm.	30
Figure 3.2:	Reconstructed image (A) and illustration (B) of BP/1/7074 in dorsal view. Scale bars equal 1cm.	33
Figure 3.3:	Photograph of left maxilla of BP/1/7074 in medial view. Scale bar equals 1cm.	34
Figure 3.4:	Photograph of left medial side of the skull of BP/1/7074 showing the bones surrounding the orbit. Scale bar equals 1cm.	36
Figure 3.5:	Photograph of right frontal and postfrontal of BP/1/7074 in dorsal view. Scale bar equals 1cm.	39
Figure 3.6:	Dorsal view of left and right parietal, and pineal opening of BP/1/7074. Scale bar equals 1cm.	42

Figure 3.7:	Reconstructed image (A) and illustration (B) of BP/1/7074 in ventral view. Scale bar equals 1cm.	44
Figure 3.8:	A) Photograph of posterior projection of the left and right vomer of BP/1/7074 which continues under the palatine in a triangular form, in lateral view; (B) photograph of position of the posterior projection of the vomer with relationship to the palatine and palatine boss. Scale bar equals 1cm.	46
Figure 3.9:	Photograph of left and right pterygoids of BP/1/7074 in ventral view. Scale bar equals 1cm.	47
Figure 3.10:	Reconstructed image (A) and illustration (B) of BP/1/7074 in occipital view. Scale bar equals 1cm.	50
Figure 3.11:	Photograph of left and right quadrate bones of BP/1/7074 in (A) anterior view; (B) posterior view; and (C) ventral view. Scale bar equals 1cm.	52
Figure 3.12:	Photograph (A) and illustration (B) of left dentary of BP/1/7074 in lateral view. Scale bar equals 1cm	53
Figure 3.13:	Dentition of BP/1/7074: (A) Photograph of incisors in ventral view; (B) photograph of canine and replacing canine of the right maxilla in medial view; (C) photograph of postcanines of the left maxilla in ventral view. Scale bars equal 1cm.	56

Figure 3.14:	Photograph of the atlas centrum of BP/1/7074 in: (A) anterior view; (B) dorsal view; and (C) posterior (B) view. Scale bar equals 1cm.	57
Figure 3.15:	Photograph and illustration of the axis of BP/1/7074 in: (A) lateral view; (B) anterior view; (C) posterior view. Scale bars equal 1cm.	58
Figure 3.16:	Photograph of the third and fourth cervical vertebra of BP/1/7074 in (A) lateral view; (B) anterior view; (C) posterior view. Scale bars equal 1cm.	59
Figure 3.17:	3-D reconstruction of BP/1/7074 in dorsal view. Scale bar equals 1cm.	62
Figure 3.18:	3-D reconstruction of BP/1/7074 in (A) left lateral view and (B) right lateral view. Scale bar equals 1cm.	63
Figure 3.19:	3-D reconstruction of BP/1/7074 in occipital view. Scale bar equals 1cm.	64
Figure 3.20:	3-D reconstruction of BP/1/7074 in ventral view. Scale bar equals 1cm.	65
Figure 3.21:	C-T slice image of the forth replacement incisor of the left premaxilla of BP/1/7074. Scale bar equals 1cm.	68
Figure 3.22:	C-T slice image of the left maxilla of BP/1/7074 showing the replacement canine and single postcanine. Scale bar equals 1cm.	69
Figure 3.23:	C-T slice image of the left dentary of BP/1/7074	

	showing the fourth replacement incisor.	
	Scale bar equals 1cm.	70
Figure 3.24:	C-T slice image of the replacement incisor of left dentary of BP/1/7074. Scale bar equals 1cm.	71
Figure 3.25:	Regression of length of the skull (tip of snout to parietal foramen) (log Variable 4) on anteroposterior length of the temporal fenestra (log Variable 7). $b_1 = 2.44$ .	74
Figure 3.26:	Regression of length of the skull (tip of snout to parietal foramen) (log Variable 4) on length of the anterior margin of premaxilla to the posterior extremity of posterior process (log Variable 13). $b_1 = 2.13$ .	74
Figure 3.27:	Regression of length of the skull (tip of snout to parietal foramen) (log Variable 4) on height of the jugal below the orbit (log Variable 21). $b_1 = 1.61$ .	75
Figure 3.28:	Regression of length of the skull (tip of snout to parietal foramen) (log Variable 4) on width of postorbital bar (log Variable 22). $b_1 = 1.71$ .	75
Figure 4.1:	Skulls and skull lengths of (A) a juvenile <i>Anteosaurus magnificus</i> (BP/1/7074) and (B) an adult <i>Anteosaurus magnificus</i> in left lateral view. Skull length is indicated for each specimen in mm. (B after Kammerer, 2011).	77

Figure 4.2: Skulls and skull lengths of the anteosaurids (A) juvenile *Anteosaurus magnificus* (BP/1/7074); (B) *Syodon biarmicum*; (C) *Titanophoneus potens*; (D) an adult *Anteosaurus magnificus* in left lateral view. Skull length is indicated for each specimen in mm. (B, C and D after Kammerer, 2011: 292).

82

## LIST OF TABLES

Table 3.1:	Summary of regressions on the length of the skull (tip of snout to parietal foramen) of <i>Anteosaurus</i> <i>magnificus</i> (Appendix A: Variable 4).	73
------------	--	----

## LIST OF ANATOMICAL ABBREVIATIONS USED

az:	anterior zygapophysis
bo:	basioccipital
bs:	basisphenoid
c:	centrum
d:	dentary
ex:	exoccipital
f:	frontal
ip:	interparietal
ipt:	interpterygoid
j:	jugal
jf:	jugular foramen
lac:	lacrimal
lt.tr.co:	lateral trochlear condyle
m:	maxilla
m.tr.co:	medial trochlear condyle
mf:	maxillary fossa
n:	nasal
na:	neural arch
nc:	neural canal
ns:	neural spine
op:	opisthotic
pal:	palatine
par:	parietal



pin:	pineal foramen
pm:	premaxilla
po:	postorbital
pof:	postfrontal
prf:	prefrontal
pt:	pterygoid
pz:	posterior zygapophysis
q:	quadrate
qj:	quadratojugal
sm:	septomaxilla
so:	supraoccipital
sq:	squamosal
t:	tabular
v:	vomer

## LIST OF INSTITUTIONAL ABBREVIATIONS

BMNH:	Natural History Museum, London, UK
BP:	Evolutionary Studies Institute, formerly Bernard Price Institute for Palaeontological Research, University of the Witwatersrand, Johannesburg, South Africa.
GMV:	Geological Museum of China, Beijing, China.
NMQR:	National Museum, Bloemfontein, South Africa.
PIN:	Paleontological Institute of the Russian Academy of Sciences, Moscow, Russia.
SAM:	Iziko, South African Museum, Cape Town, South Africa.
UFRGS:	Universidade Federal do Rio Grande do Sul, Porto Alegre, Brazil.

## LIST OF STATISTICAL ABBREVIATIONS

$b_1$ :	slope
$\log b_0$ :	y intercept
$n$ :	sample size
$P_{(iso)}$ :	probability
$R^2$ :	determination coefficient
RMA:	Reduced Major Axis

## CHAPTER ONE: INTRODUCTION AND LITERATURE REVIEW

### 1.1 General Introduction

Although a wide diversity of tetrapods are known from Middle Permian deposits, therapsids were the most abundant, and dinocephalians are particularly well represented. They were the first large land-living tetrapods and have been found in Middle Permian rocks of Brazil (Langer, 2000; Cisneros *et al.*, 2012), China (Li and Cheng, 1995; Cheng & Ji, 1996; Cheng & Li, 1997; Li *et al.*, 1996), Russia (Efremov, 1954; Orlov, 1958; Ivachnenko, 1995; Ivachnenko, 2000), South Africa (Boonstra, 1963; Rubidge, 1991; Rubidge, 1994; Rubidge & van den Heever, 1997; Kemp, 2005; Kammerer, 2011), Zimbabwe (Lepper *et al.*, 2000), and most recently Tanzania (Simon *et al.*, 2010).

The rocks of the Karoo Supergroup of South Africa preserve a vast diversity of Permian-Jurassic tetrapods, and eight biozones have been defined after this fauna. The *Tapinocephalus* Assemblage Zone of the Beaufort Group has many tetrapod taxa, amongst the highest, the Dinocephalia, making up approximately 30.7% of all fauna, surpassed only by the Dicynodontia, which account for 30.9% (Smith *et al.*, 2011). Dinocephalians were clearly abundant during this time, and interestingly comprise carnivores, herbivores and omnivores, essentially occupying all three ecological feeding niches (Boonstra, 1969; Nicolas and Rubidge, 2010). Although dinocephalians made up a large percentage of the

Middle Permian terrestrial tetrapod fauna they became extinct at the close of the *Tapinocephalus* Assemblage Zone (Boonstra, 1971; Day, 2013).

## **1.2 Historic Review of the Anteosauridae**

By the 1950's the infraorder Dinocephalia was considered to comprise six families, namely the Estemmenosuchidae, Brithopodidae, Anteosauridae, Titanosuchidae, Tapinocephalidae and the Styracocephalidae (Boonstra, 1963; Kemp, 1982). King (1998) later reclassified these as subfamilies within three families; Estemmenosuchidae, Brithopodidae and Titanosuchidae. Of these three families recognised by King (1988), only the Estemmenosuchidae have not been found in Africa (Rubidge, 1991). Watson and Romer (1956) originally separated the herbivorous and carnivorous dinocephalians into two separate groups based on the premise that the carnivorous forms were more advanced. Later the Dinocephalia were recognised as a monophyletic taxon due to the similarities between the carnivorous and herbivorous forms, and the carnivorous Anteosaurids were considered to be plesiomorphic (Kemp, 2005).

The characters that now define the Dinocephalia are: 1) Incisor teeth bearing a slight heel on the lingual face at the base of the crown. 2) Uppers and lowers interdigitate, a feature which is also present in some biarmosuchians and gorgonopsians. 3) Enlargement of the temporal fenestra in such a way that temporal musculature attachment expands upwards and forwards onto the dorsal surface of the parietal and postorbital bones. 4) Forwards shift in the jaw

articulation, shortening the length of the jaw. 5) A strong tendency towards thickening of the skull bones, to the point of heavy pachyostosis in many forms (Kemp, 2005).

Since King's (1988) phylogenetic relationships of the Dinocephalia (Figure 1.1), little has changed and today four families of Dinocephalia are currently recognized: Estemmenosuchidae, Anteosauridae, Tapinocephalidae and Titanosuchidae (Rubidge, 1991; Kammerer, 2011).

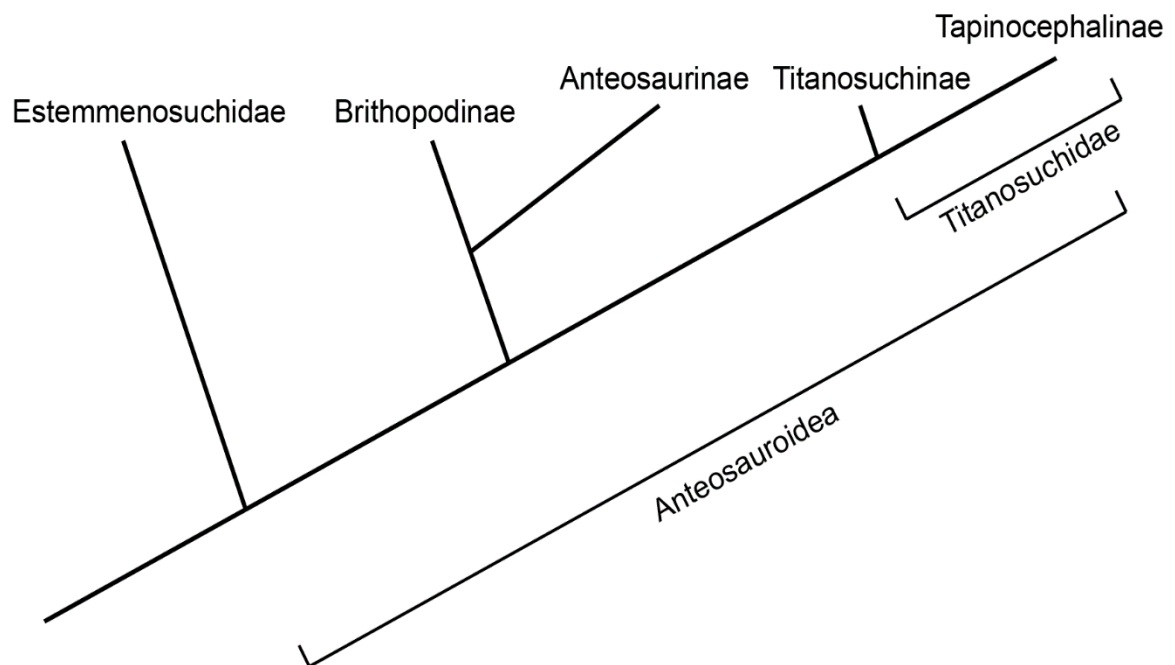


Figure 1.1: Cladogram showing the phylogenetic relationships of the main dinocephalian groups (King, 1988).

Amongst the carnivorous dinocephalians only two genera, *Australosyodon* and *Anteosaurus* are recognised from the Karoo rocks of South Africa (Kammerer,

2011). *Australosyodon* is the most basal (Rubidge, 1994; Kammerer, 2011), and like the Russian and Brazilian basal anteosaurids, is relatively small. By contrast *Anteosaurus* is a particularly large animal and was a formidable carnivore.

Phylogenetic analysis of anteosaurs recovers a monophyletic Anteosauridae containing two major clades, Syodontinae (including *Australosyodon*, *Notosyodon* and *Syodon*) and Anteosaurinae (containing *Anteosaurus*, *Sinophoneus* and *Titanophoneus*) (Kammerer, 2011; Liu, in press; Figure 1.2). The Russian taxa *Archaeosyodon* and *Microsyodon* represent the most basal anteosaurs (Kammerer, 2011; Liu, in press).

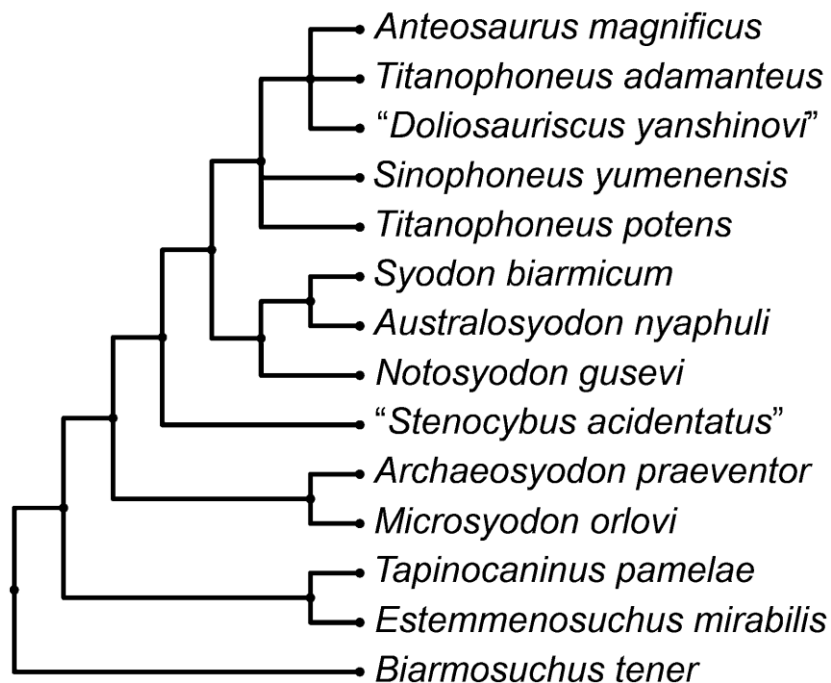


Figure 1.2: Cladogram of anteosaurian relationships (Kammerer, 2011).

*Doliosauriscus yanshinovi* is regarded as a junior synonym for *Titanophoneus potens*.

Anteosaurian skulls present many similarities when compared with those of large-bodied predatory taxa such as tyrannosaurid dinosaurs. Anteosaurines in particular exhibit characters associated with handling large prey items and possibly bone-crushing (Kammerer, 2011). Postcanine morphology of the anteosaur is believed to change over the course of ontogeny (Kammerer, 2011). Although a taxonomic reappraisal of the anteosaur has been conducted by Kammerer (2011), a detailed description of the cranial morphology of *Anteosaurus* still needs to be done.

Efremov (1954) initially named the family Brithopodidae referring to the Russian *Brithopus*, and the better known *Syodon* and *Titanophoneus*, and the name was used in work later carried out on the group (such as Romer, 1956, 1966; Watson and Romer, 1956; Olson, 1962; Boonstra, 1963; Kemp, 1982; Tchudinov, 1983; Sues, 1986; King, 1988; Battail and Surkov, 2000) to refer to non-*Anteosaurus* anteosaur (Kammerer, 2011). Later the family Brithopodidae was referred to as Brithopidae (Boonstra, 1972) and Brithopia (Kemp, 1982). Hopson and Barghusen (1986) believed that the name Brithopodidae should be withdrawn and that the Russian taxa *Syodon*, *Titanophoneus* and *Doliosauriscus* should be placed under the Anteosauridae. Hopson and Barghusen (1986) erected Anteosaurini which contained *Doliosauriscus* and *Anteosaurus*, Anteosaurinae containing *Titanophoneus*, *Doliosauriscus* and *Anteosaurus*, and Anteosauria – a higher taxon level for Anteosauridae to compliment Tapinocephalia. King (1988) placed the family Brithopidae and Titanosuchidae in the superfamily Anteosauroidae. Ivakhnenko (1994) established the family Syodontidae to include *Syodon*,



*Notosyodon* and *Archaeosyodon*, and considered the Brithopodidae an invalid family.

### 1.2.1 Anteosaurids from South Africa

The holotype specimen of *Anteosaurus magnificus* (BMNH R3595) was originally referred to as *Titanosuchus ferox* (Owen, 1879) and was later made the type specimen of the new species *Anteosaurus magnificus* (Watson, 1921). Since Watson (1921) established *Anteosaurus magnificus*, a great number of new specimens have been described from the Beaufort Group of South Africa and many taxa have been synonymized with the name.

Boonstra (1954a) provided a detailed description of the *Anteosaurus* skull and in doing so named a number of different *Anteosaurus* species, namely *A. acutirostris*, *A. crassifrons*, *A. major*, *A. laticeps*, *A. cruentus* and *A. levops*. In addition he referred a skull fragment, which was previously described as the type specimen of *A. minor* by Broom (1929), to the genus *Pseudanteosaurus minor*, and placed Broom's *A. minor* as a new species, *A. minusculus*. Later, Boonstra (1954b) described *Micranteosaurus parvus* and *Paranteosaurus primus* (Boonstra 1954c) and formally considered the taxa *Dinosuchus* and *Titanognathus* as *Anteosaurus*. Boonstra (1969) later synonymized most of the South African anteosaurids with *Anteosaurus magnificus* and kept the genus *Paranteosaurus primus*. Boonstra (1969) decided that the differences between *Anteosaurus magnificus* and *A. cruentus*, *A. levops*, *A. minor*, *A. minusculus*, and

*Micranteosaurus parvus* can be attributed to ontogenetic variation. He also recognised the differences between *A. abeli*, *A. acutirostris*, *A. crassifrons*, *A. laticeps*, *A. major*, *A. vorsteri* and *A. magnificus* as the result of taphonomic distortion or differences in the amount of pachyostosis that they exhibited.

*Australosyodon*, described by Rubidge (1994), is a medium sized dinocephalian preserved with the lower jaw. The specimen (NMQR 3152) is the only specimen of its genus and is most closely related to the Russian genus *Syodon*. NMQR 3152 (*Australosyodon*) lacks the apomorphic characters of *Anteosaurus* however is clearly an anteosaurid dinocephalian. Thus it is believed that this specimen is more closely related to the primitive anteosaurid dinocephalians from Russia. *Australosyodon* was compared to the Russian ‘brithopodids’, discussed later in this chapter, such as *Australosyodon*, *Archaeosyodon*, *Doliosauriscus*, *Notosyodon*, *Syodon* and *Titanophoneus*. Rubidge (1994) found *Australosyodon* to be a very primitive anteosaurid, and thus the first basal anteosaurid from the southern hemisphere, closely resembling *Syodon* but differing in the following regards: the palatine bosses of *Australosyodon* do not protrude as far ventrally as those of *Syodon*; no teeth are present on the lateral flange of the pterygoid in *Australosyodon*; the pterygoid boss of *Australosyodon* is larger than that of *Syodon*; the canine differs from that of *Syodon* as it is not rounded in cross section; the teeth on the maxilla and dentary are less robust than that of *Syodon*; contact of the frontal bone on the dorsal border of the orbit is slightly greater than the condition seen in *Syodon*; and the longitudinal medial ridge extends down the midline of the frontal but differs from that of *Syodon* in that it expands laterally to

form a prominent medially situated boss above the orbits before continuing posteriorly as a ridge up until the pineal boss (Rubidge, 1994).

*Micranteosaurus parvus* (SAM-PK-4323) was described by Boonstra (1954b) on the basis of a snout and associated postcranial elements. The snout is almost identical to large *Anteosaurus* specimens, however is approximately one third of the size. Boonstra (1969) argued that *Micranteosaurus* is a juvenile individual and that the characters which set it apart from *Anteosaurus magnificus* are influenced solely by ontogenetic factors. Thus SAM-PK-4323 is the smallest individual of *Anteosaurus* known.

### **1.2.2 Anteosaurids from Russia**

The family Brithopodidae was previously used to include the anteosaurid dinocephalians which are widespread in Permian rocks of the Cis-Uralian region of Russia (Efremov, 1954; Tchudinov, 1968) and includes those of both the Cis-Uralian Dinocephalian Complexes and the Isheevian Dinocephalian Complex (Olson, 1962).

The following diagnosis has been given for the Russian anteosaurids (Olson, 1962: 57): “A group of the most primitive carnivorous dinocephalians. Skull high and narrow. Palatal choanae posterior with anterior margins between the canines. Teeth on the pterygoid flange reduced. Marginal teeth of three types: anterior, large; canine, very large; cheek teeth either trenchant and tending to decrease in number or declining in size from anterior to posterior. Number of cheek teeth

about ten. Premaxillary step present. Temporal opening open above (postorbital bone and bar large, modified to produce area for origin of superficial adductor jaw muscles on outer surface of skull). Pineal tuberosity thick and high, with large canal for parietal organ. Zygoma narrow. Shoulder girdle with narrow interclavicle, clavicle, and scapular blade. Humerus with both epicondylar foramina. Femur slender and curved.”

A short review of the different Russian anteosaurid genera is presented:

*Archaeosyodon* described by Tchudinov (1960) is from the Ezhovo locality, Kazanian, Cis-Uralian of Russia. Its location is believed to correspond to the Permian, where many of the Russian anteosaurs have been discovered.

*Archaeosyodon* is described as being a large carnivorous anteosaurid with a broad zygomatic region. The holotype (PIN 1758/3) has a primitive palate especially with regards to the arrangement of the palatal teeth (Olson, 1962).

*Syodon efremovi* was first described as *Cliorhizodo* by Efremov (1940) but later Orlov (1958) assigned the specimen to the genus *Syodon*. The holotype (PIN 157/2) is from the Isheevo complex of Russia. A second species of *Syodon*, *Syodon biarmicum*, was collected from the Copper Sandstones near Isheevo. The difference between the two species relates to size as well as dentition (Olson, 1962). Noticeably the temporal opening of *Syodon* is most similar to that of *Titanophoneus* in which the postorbital bone is large and thick and provides an area for origin of part of the superficial adductor musculature, on the outer dermal surface of the skull (Olson, 1962). *Syodon* is considered to be the least derived

anteosaurid based on the fact that it lacks a boss on the angular adjacent to the dentary (Hopson and Barghusen, 1986). This feature is also absent in the primitive South African anteosaurid *Australosyodon* (Rubidge, 1994).

*Brithopus* was described by Efremov (1954) from material found in the Copper Sandstones near Isheevo. This genus most resembles *Titanophoneus*, however the cranial bones seem to be more ossified and more massive (Olson, 1962).

The description of *Titanophoneus potens*, by Orlov (1958), was based on the holotype (PIN 157/1) from Isheevo. The temporal fenestra is similar to that of *Syodon* in that it is very high and narrow. The pineal opening is positioned on a chimney above the skull roof. This feature is very characteristic of the Russian anteosaurs. The temporal – parietal region exhibits the most characteristic Russian anteosaurid features which include: deep orbits with the expansion of the postorbital over and behind the orbit, and the development of a very high occiput, a feature which Olson (1962) attributes to muscle patterns of both the adductor system and cervical region.

*Doliosauriscus* is the largest anteosaurid genus from Isheevo and the holotype comprises a skull and relatively complete skeleton. Described by Orlov (1958), the postorbital bone of this genus (PIN 157/3) is very large and forms a strong bar between the orbit and the temporal opening. Olson (1962) notes that as in the other ‘brithopodids’, the adductor musculature of the jaws of *Doliosauriscus* took origin on part on the outer surface of the postorbital. The large size of the skull

seems to obscure the typical ‘brithopodid’ features of the temporal and parietal regions, however the overall cranial structure greatly resembles that of *Titanophoneus* and *Syodon*. *Doliosauriscus* has recently been synonymised with *Titanophoneus potens* (Kammerer, 2011).

*Notosyodon gusevi* described by Tchudinov (1968) is believed to be closely related to *Syodon* and manifests many similarities with *Syodon*, such as its general overall configuration and the position of its orbits and temporal fenestra. However *Notosyodon* differs from *Syodon* in its general greater massiveness and considerably greater skull size (Tchudinov, 1968). *Notosyodon* may have possibly been an omnivorous dinocephalian and shows that the later anteosaurids such as *Syodon* and *Titanophoneus*, which were considered highly mobile predators based on their morphology, differ from the titanosuchid dinocephalians (Tchudinov, 1968).

*Microsyodon orlovi* was described by Ivachnenko (1995) on the basis of an isolated right maxilla (PIN 4274/13). *Microsyodon* is based on fragmentary material and was first considered to be a titanosuchid (Ivachnenko, 1995) however it has been shown to be an anteosaur based on the convex ventral margin of its maxilla (Kammerer, 2011). It can be distinguished from all other anteosaurs by a maxillary precanine, and all anteosaurs except *Archaeosyodon* and *Syodon* by possessing a strongly recurved canine (Kammerer, 2011). Kammerer (2011) believes that the shape and angulation of the precanine suggests that it is not a replacement canine and the small size of this specimen suggests that it is a

juvenile. It has been suggested that *Microsyodon* could be a juvenile representative of *Archaeosyodon* based on similar morphological characteristics, however it must be noted that *Microsyodon* was retrieved from an earlier stratigraphic assemblage than *Archaeosyodon* and thus is believed to be a valid anteosaurid taxon (Kammerer, 2011).

### **1.2.3 Anteosaurids from Brazil**

The first record of dinocephalians reported from South America were recovered from the Rio do Rasto Formation of the Paraná Basin in Brazil (Langer, 2000). Both Brithopodinae and Titanosuchidae have been recognised from this location, however the specimens comprise mostly isolated teeth and one single bone. Most notably, Langer's (2000) find included an incisiform tooth, most similar to that of the titanosuchids and incisors most similar to the anteosaurids.

More recently the genus *Pampaphoneus*, an anteosaurid dinocephalian, was described from the Morro Pelado Member of the Rio do Rasto Formation, Brazil, and is proposed to be Guadalupian in age (Cisneros *et al.*, 2012). The specimen (UFRGS PV386P) is a complete medium-sized anteosaurid skull with little pachyostosis, which differs from other anteosaurids in having a premaxilla that bears only four teeth; a squamosal-jugal process that surpasses the anterior-most margin of the temporal fenestra; and the presence of a shallow, elliptical, angular boss (Cisneros *et al.*, 2012). *Pampaphoneus* can be distinguished from all anteosaurids, except *Syodon*, by the presence of at least eight short, bulbous

postcanines bearing front and back serrations. Its skull size is shorter than that of all anteosaurines but larger than all syodontines and most similar to that of the Russian *Archaeosyodon*. Notably *Pampaphoneus* has a long recurved canine which is most similar to that of *Syodon* and *Archaeosyodon*. Phylogenetic analysis placed *Pampaphoneus* as the most basal syodontine, a clade formed by *Notosyodon*, *Syodon*, and *Australosyodon* (Cisneros *et al.*, 2012).

#### **1.2.4 Anteosaurids from China**

A primitive anteosaurid was recovered from the Xidagou Formation at Yumen in the Gansu Province in China. Li *et al.* (1996) considered this find to be an anteosaurid dinocephalian because the specimen has a jaw articulation which is positioned slightly anteriorly and has little pachyostosis. Re-examination of the anteosaurids from Russia, South Africa and China found two additional autapomorphies of the Anteosauridae. These are 1) a depression of jaw adductor musculature on the skull roof lateral to the pineal boss and immediately anterior to the temporal fenestra, and 2) a basisphenoid with bulbous lateral ridges on either side, which converge anteriorly to form a single midline ridge extending anteriorly as far as the interpterygoid vacuity (Li *et al.*, 1996).

*Sinophoneus yumenensis* was described by Cheng and Ji (1996) and this specimen (GMV1601) has been shown to be a large, primitive anteosaurid. It differs only slightly from the more derived *Anteosaurus* in lacking a prominent postfrontal boss overhanging the dorsal border of the orbit; possessing a long series of



postcanine teeth; and having the flat skull roof with in the pre- to postfrontal region (Cheng and Ji, 1996).

Shortly after the description of *Sinophoneus*, another primitive dinocephalian *Stenocybus acidentatus* was described from Yumen in the Gansu Province of China. In contrast to *Sinophoneus* this genus is a small-sized dinocephalian, without cranial pachyostosis (Cheng and Li, 1997). These authors note that *Stenocybus* is more similar to primitive therapsids (such as biarmosuchia) than to dinocephalians, however features such as interlocking incisors bearing distinct lingual heels, and the depression receiving the lower jaw adductor presenting anterolateral to the parietal foramen on the dorsal surface of the skull, suggests that *Stenocybus* is more closely related to dinocephalians. Kammerer (2001) considers *Stenocybus* to be a juvenile of *Sinophoneus*.

### **1.3 Dentition and Tooth Replacement**

The dentition of the Dinocephalia can be distinguished from that of all other orders of the Therapsida by the unique intermeshing incisors, although some biarmosuchians are more recently believed to potentially possess this character as well (Sidor and Welman, 2003). The upper and lower incisors of Dinocephalia intermesh in occlusion, and in Titanosuchia, the lower canine passes in front of the upper canine to intermesh between the last upper incisor and upper canine (Boonstra, 1962). In contrast the usual condition in other therapsids sees the upper incisors passing labially of the lower incisors (Boonstra, 1962; King, 1988). Most

dinocephalians present a talon-and-heel tooth morphology of the incisors which is distinct from all other therapsids (King, 1988).

The incisors of the Anteosauridae are usually elongate conical teeth. Romer (1961) noted that in *Anteosaurus* and its relatives the incisors lack the posterior “heel” seen in other dinocephalians, however Boonstra (1962) believed that this “heel” may be incipient in some forms of anteosaurids.

The first concerted attempt to explain tooth replacement of basal therapsids was made by Parrington (1936) in his paper on the tooth-replacement in Theriodonts. Since then numerous studies have been undertaken to explain the tooth replacement strategies of the bauriamorphs (Crompton, 1962), gorgonopsians (Kermack, 1956), and the cynodonts and dicynodonts (Hopson, 1964). The first study pertaining to dinocephalian tooth replacement was undertaken by Janensch (1959) and later Boonstra (1962), both looking at the dentition of the Titanosuchid *Jonkeria*. Boonstra (1962) produced five sections of the dentition of *Anteosaurus abeli* (later synonymised with *Anteosaurus magnificus*) and found that tooth replacement occurred for incisors, canines and postcanines but is however less frequent for the canines. *Anteosaurus* shows evidence of at least two replacement sets of canines and postcanines, and at least three sets for incisors (Boonstra, 1962). He concluded that there is no evidence that replacement of teeth in the anteosaurids terminates. Thus this process was believed to be continuous throughout the dinocephalian’s life.

In the incisors, canines and postcanines of *Anteosaurus* the replacing tooth erupts lingually of the existing tooth. Boonstra (1962) states that each replacing tooth follows the previous generation of teeth independently, meaning that at any time, except for the initial teeth, the teeth are never of the same age or generation. This trend is most noticeable for the incisors, as very distinct stages of wear and development are apparent (Boonstra, 1962). Boonstra (1962) found that anteosaurid incisors replace in a way similar to that of the titanosaurs, however the anteosaurids show a different method of eruption. Titanosaurs exhibit the development of pockets in the lingual face of the alveolar wall of the functioning incisor for the emergence of the replacing incisor, but this character has not been observed in the anteosaurids.

This pioneering work on tooth replacement patterns in *Anteosaurus* has never been repeated, despite the fact that Boonstra (1962) acknowledges that tooth replacement of the anteosaurids has not been adequately addressed. The discovery of a juvenile anteosaurid, combined with recent refinement of Microfocus X-ray computed tomography (CT) scanning technology provides a good opportunity to study dental replacement patterns in a juvenile *Anteosaurus*.

## CHAPTER TWO: MATERIALS AND METHODS

### 2.1 Specimens

The fossil cranial material required for this study is curated in various South African museums, and the specimens used are listed below. However this study is based mainly on a single, and almost complete skull of a juvenile *Anteosaurus* (BP/1/7074) which was collected in 2011 from the Abrahamskraal Formation (*Tapinocephalus* Assemblage Zone, in the mudstone L of Jirah, 2013) of the Beaufort Group, near Merweville, (32° 26.071 S, 21° 26.654 E) on the farm Bullekraal (farm number 251) in the Beaufort West district. Other specimens which were studied for comparative and allometric purposes are:

BP/1/1369: *Anteosaurus magnificus* – well preserved specimen consisting of the skull and lower jaws;

BP/1/7074: *Anteosaurus magnificus* – well preserved juvenile skull with a portion of the lower jaw and cervical vertebrae;

SAM 11577: *Anteosaurus vorsteri* – well preserved large skull with palate;

SAM 4340: *Anteosaurus abeli* – (cotype) laterally compressed skull with a complete left lateral side;

SAM K1683: *Anteosaurus* sp. – skull with left lateral side well preserved;

SAM 9329: *Anteosaurus acutirostris* – (holotype) well preserved skull with large boss below postorbital bar;

SAM 11302: *Anteosaurus crassifrons* – left lateral side of skull and lower jaw, specimen is lacking the palate;

SAM 11492: *Anteosaurus levops* – (holotype) incomplete specimen which is partially prepared;

SAM 11694: *Anteosaurus cruentus* – (holotype) well preserved and undistorted skull without the lower jaw;

SAM K284: *Anteosaurus* sp. – well preserved specimen with fully prepared skull and palate.

## **2.2 Preparation**

Preparation of the specimen (BP/1/7074) was undertaken by Mrs. Cynthia Kemp in 2012 at the Evolutionary Studies Institute, University of the Witwatersrand. All preparation was mechanical and was undertaken by using a Desoutter VP2-X airscribe fitted with tips of tungsten carbide. Paraloid, diluted with acetone, was used as an adhesive. Because the specimen is a juvenile individual (see later), during the preparation process most of the unfused bones fell apart at their sutures. This resulted in approximately 45 cranial fragments and created a wonderful opportunity for a detailed description of a juvenile *Anteosaurus* skull. Some of these elements, for example, the left prefrontal, frontal, postfrontal, postorbital and squamosal were fitted and glued back together. Other elements, which were distorted during the fossilization process, could not be fitted together in this manner. These elements were left separately and prepared, if possible, by removing surrounding matrix.

### **2.3 Microfocus X-Ray Computed Tomography (CT) Scanning and Segmentation**

In 1895 Wilhelm Conrad Röntgen discovered X-rays at the Institute of Physics of the University of Würzburg. Röntgen found that from a discharge tube and the transport of electricity in gases at high voltages, a penetrating radiation occurred (Haase *et al.*, 1997). In the 1900s this discovery by Röntgen was used extensively for medical purposes and it was not until the 1950s until an X-ray image intensifier was created, which allowed the display of the X-rays using a TV monitor. Once computed tomography was developed by the 1960s it was clear that it has huge medical advantages, as well as the opportunity to apply this technology to fields such as palaeontology, sedimentology, petrology, and soil science.

Computed tomography was originally designed and used by Hounsfield (1973) to obtain cross-sectional images of the human head. Later Ledley *et al.* (1974) further developed the application for examination of other body regions. The first application of computed tomography for the use in a palaeontological context was undertaken by Fourie (1974) and the success of this application lead to later use of this technique such as Conroy and Vannier (1984) who used it to examine four primate skulls which had been filled with hardened matrix. The application was found to be a reliable means of dissecting a specimen virtually with non-invasive techniques. Since Conroy and Vannier's (1984) application, computed tomography has been used in a wide variety of geoscience subdisciplines. These

include the non-invasive assessment of *Archaeopteryx* by Haubitz *et al.* (1998), Ketcham and Carlson's (2001) geological applications which included interior examination of fossils and meteoritics; textural analysis of igneous and metamorphic rocks; geometric description and quantification of porosity and permeability in rocks and soils, Carlson *et al.* (2003) non-destructive analysis for geological specimens, Schwartz *et al.* (2005) scanning of vertebrate remains with comparison to neutron scanning data, and DeVore *et al.* (2006) studies of palaeobotanical remains. X-ray has been used to investigate arthropod structures (Betz *et al.*, 2007) and even the examination of fossil burrow casts (Fernandez *et al.*, 2013). Microfocus X-Ray Computed Tomography (CT) Scanning has over the years therefore proved to be invaluable to palaeontologists for the non-destructive application and analysis of fossilized material and has reproduced remarkable results. This study represents the first CT scan of an anteosaurid dinocephalian for non-invasive analysis and reconstruction.

BP/1/7074 was scanned using Microfocus X-ray computed tomography (CT) with a Nikon Metrology XTH 225/320 LC dual source industrial CT system. Due to the size constraints of the system and the relatively large size of the specimen, seven individual scans were completed, with each scan incorporating five to ten elements or fragments. Elements and fragments to be scanned were packed into specially constructed Perspex tubes, which were filled with bubble wrapping and then the elements that needed to be scanned. Each scan was completed at 190KV and 105 $\mu$ A. Three thousand projections were taken at one frame per second, averaging two frames per second. A 2.4mm copper filter was used during the

scanning. Data from each scan was uploaded to the Virtual Imaging Processing (VIP) Laboratory at the Evolutionary Studies Institute, University of the Witwatersrand, Johannesburg, for analysis. Scans were reconstructed using VSG's Avizo® Fire. Each reconstructed scan totalled approximately 30GB (gigabytes), and was segmented using the same software. Scans which were completed as part of a compilation of two scans, were stitched together using Volume Graphics' VGStudio Max. Reconstructed scans were exported as RAW TIFF stacks and segmented as RAW TIFF stacks.

Segmentation was selective, as a few elements needed to be separated by segmentation. These included three incisors, one canine and the segmentation of the left premaxilla and right premaxilla. Segmentation was completed manually using VSG's Avizo® Fire and Wacom graphics tablets. Once segmentation was completed, elements were exported as PLY (Polygon File Format, also known as the Stanford Triangle Format) file formats.

## **2.4 3-D Reconstruction**

A 3-D reconstruction of BP/1/7074 was accomplished using VSG's Avizo® Fire. Each element exported to the PLY format was read in to memory as a surface file. These surface files were combined as separate elements by rotation and alignment. Reconstruction was accomplished by first reconstructing the elements of the skull roof, then the palate and finally the occiput. These separate reconstructions were brought together to complete an entire reconstruction.



Elements which were missing or damaged were replaced by mirroring the opposing complete element. In this way, much of the right side of the specimen was reconstructed from the left, and the antero-postero distortion could be corrected.

## **2.5 Tooth Replacement**

To evaluate the pattern of tooth replacement occurring in BP/1/7074, CT data was read as a RAW TIFF stack and manually assessed for replacing teeth. These teeth can be found by using a coordinate system within VSG's Avizo® Fire and running consecutively through each CT TIFF image.

## **2.6 Allometric Analysis**

Because of the availability in South African museum collections of a number of *Anteosaurus* skulls of different sizes which have been recently prepared, an allometric analysis was performed using PAST v 2.17C (Hammer *et al.*, 2001). The measurements used in this study were taken from a study by van den Heever and Rubidge (in prep). A total of forty measurements were taken from fifteen specimens of *Anteosaurus* from different institutions, however most of the specimens included in the allometric analysis are not associated with postcranial material, and thus only cranial measurements were recorded and used in this study. A major problem is that, because of the fragmentary nature of most of the skulls, it was difficult to put together a set of measurements which could be

compared in all the specimens. As a result specimens which did not afford sufficient data were removed from the analysis. Thus a total of eleven specimens and twenty-three measurements were finally analysed. Measurements were log transformed and the method of Reduced Major Axis (RMA) was used. In the analysis  $b_0$  is the y-intercept and  $b_1$  the slope of the line (coefficient of allometry). When coefficients of allometry are statistically different, and are either greater or less than expected by isometry, positive or negative allometry occurs.

Measurements were taken using a sliding Vernier calliper. The different measurements taken are presented in Appendix A. A table of the measurements for each specimen is recorded in Appendix B. To eliminate the effects of distortion during the fossilisation process, measurements of BP/1/7074 were taken digitally on the reconstructed skull in Avizo® Fire. Measurements used in the allometric analysis are showed in Figure 2.1.

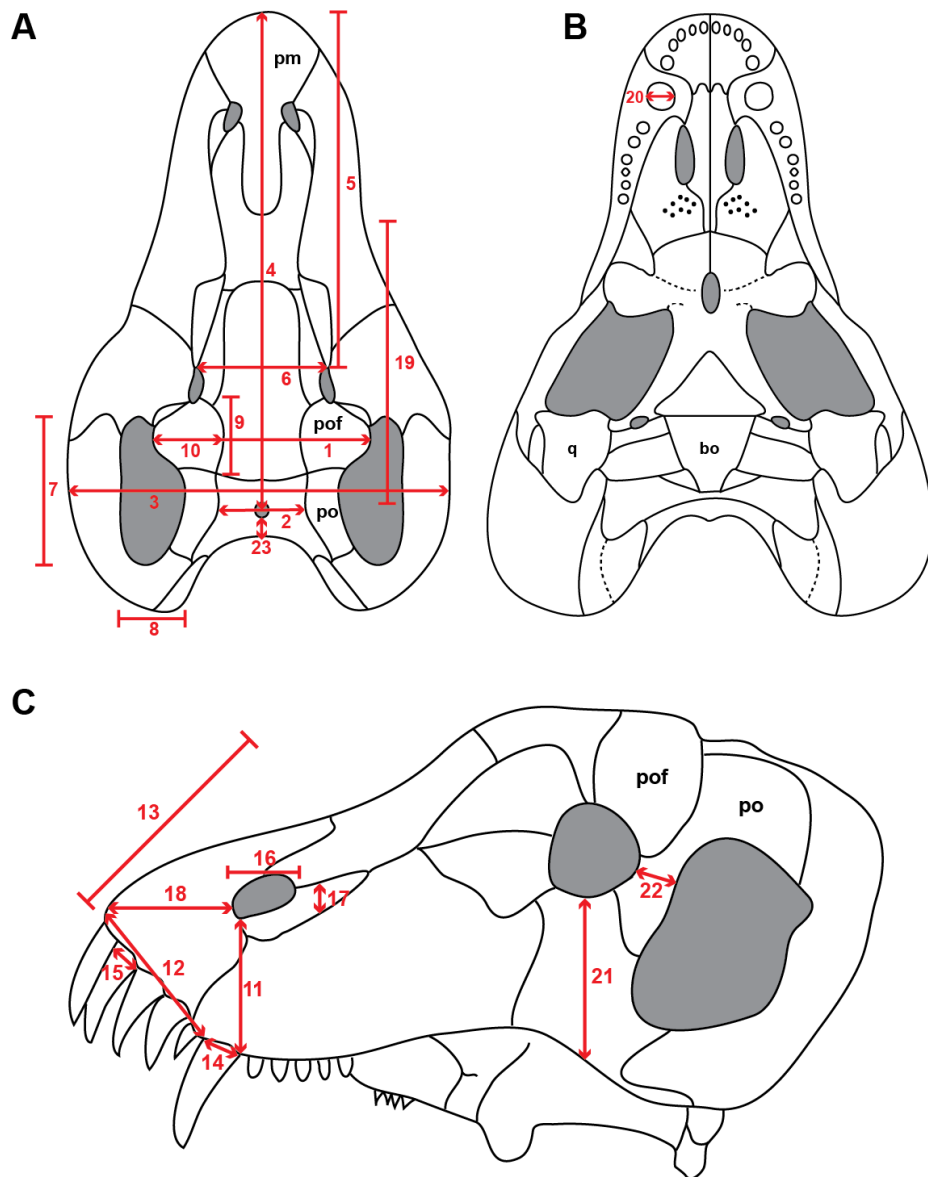


Figure 2.1: Illustration of the skull of *Anteosaururus* showing the measurements used in the allometric analysis. (A) dorsal view; (B) ventral view; and (C) lateral view. Redrawn after Boonstra (1969).

## CHAPTER THREE: RESULTS

### 3.1 Systematic Palaeontology

SYNAPSIDA Osborn, 1903

THERAPSIDA Broom, 1905

DINOCEPHALIA Seeley, 1894

ANTEOSAURIDAE Boonstra, 1962

ANTEOSAURINAE Boonstra, 1954

*ANTEOSAURUS MAGNIFICUS* Watson, 1921

**Holotype.** BMNH R3595, a partial skull

**Age.** Middle Permian (*Tapinocephalus* Assemblage Zone, Abrahamskraal Formation, Beaufort Group).

**Diagnosis.** (After Kammerer, 2011) *Anteosaurus magnificus* can be distinguished from all anteosaurs other than the two species of *Titanophoneus* on the basis of an angular boss, heavily pachyostosed skull roof including a massive frontal boss, concave alveolar margin of the precanine region, concave dorsal snout profile, posterolateral cant of the posteriormost upper postcanines, and anteroventrally-rotated suspensorium. *Anteosaurus* can be distinguished from *Titanophoneus* on the basis of an oval angular boss and the presence of ‘brow horns’ formed by the massively pachyostosed postfrontals.

**Comments.** The juvenile form of *Anteosaurus* lacks a heavily pachyostosed skull, frontal boss and ‘brow horns’ and possess a shorter snout compared to skull length than that of the adults. Juveniles can be further distinguished from the adults based on a short suborbital portion of the jugal and a reduced angulation of the skull roof. The lateral edges of the vomer of juveniles curve medially similar to the situation of *Syodon*, whereas in adults it extends ventrally.

## 3.2 Description

### 3.2.1 General Comments

The skull of specimen BP/1/7074 (Figure 3.1) is well preserved on the left side but is missing elements on the right which were lost prior to fossilisation. The mandible is incomplete and only the anterior portion of the left side is preserved. Although the skull is reasonably complete, the various elements of the skull have come apart at the sutures such that the skull comprises forty-five separate elements. In right lateral view it is evident that the orbit is relatively large compared to the temporal opening. Because of the fact that BP/1/7074 has a relatively large orbit in relation to the size of the skull, the sutures are not fused and because the skull is small, it is considered to be a juvenile, and is most probably *Anteosaurus* as will become evident later.

The excellent preservation of unfused cranial bones provides a unique opportunity to provide a detailed description of all the cranial elements of an anteosaurid dinocephalian. The adult form of *Anteosaurus* has a skull length of more than 700mm with a maximum width of approximately 600mm (van den Heever and Rubidge, in prep), in contrast specimen BP/1/7074 has a total skull length of 280mm. As Boonstra (1954c) points out, most *Anteosaurus* skulls are distorted as the result of post mortem deformation and this poses a difficulty in determining the correct skull measurements. When comparing *Anteosaurus* with other Dinocephalia it is apparent that the snout of *Anteosaurus* is relatively high and narrow relative to the orbital region and the skull has a pronounced lateral flare

(van den Heever and Rubidge, in prep). This means that the widest point of an *Anteosaurus* is across the squamosals.

Specimen BP/1/7074 exhibits minimal pachyostosis, and that which is present is evident only on the postfrontal and postorbital bones. This is in contrast to adult specimens which have a larger amount of pachyostosis on the postfrontal boss as well as on the frontals.

*Anteosaurus* can be distinguished from all other anteosaurid genera, other than *Titanophoneus*, by the presence of an angular boss and a heavily pachyostosed skull roof, which includes a massive frontal (Kammerer, 2011). In some specimens the thickened postorbital bar forms a pronounced boss on its dorsal side. Slight thickening of the postorbital is present in BP/1/7074 but not to the extent that it forms a prominent boss. Boonstra (1954a) noted an elongate swelling forming a prominent overhang on the jugal of larger specimens and also described additional bosses on the jugal and angular, as well as around the parietal foramen. In the largest specimens of *Anteosaurus* the postfrontal forms a large overhang in the form of a boss over the posterodorsal border of the orbit. This feature, although only in an incipient form, is noticeable in specimen BP/1/7074.

Kammerer (2011) states that of the known specimens of *Anteosaurus* there is a significant range and variation of both cranial proportions and the extent of pachyostosis. He considers that this variation in cranial proportions and pachyostosis can be ascribed to ontogenetic factors. For example, smaller skulls

such as SAM-PK-11492 and SAM-PK-K284, have smaller horns and bosses than those of larger *Anteosaurus* specimens. Even smaller specimens such as AMNH 2224 seem to lack pachyostosis all together, however there are exceptions such as SAM-PK-K360 and BP/1/1369 (very large specimens of *Anteosaurus*) which lack a frontal boss (Kammerer, 2011).

### **3.2.2 Skull Roof**

The premaxilla forms the anterior part of the snout and makes up the anterior, dorsal and anteroventral border of the external naris. It extends posterodorsally beyond the posterior border of the external nares. A long anteroposterior sutural contact with the large paired nasals is visible dorsally, and ventrolaterally the premaxilla makes sutural contact with the maxilla. In left lateral view a deep fossa is present at the contact with the premaxilla and maxilla, just above and posterior to the last upper incisor. A smaller, shallower fossa is present anteriorly, positioned directly above the last upper incisor. Sutural contact between the premaxilla and maxilla is also visible mediolaterally with a jagged suture which runs down the side of a bulbous canine root within the maxilla. The left premaxilla of BP/1/7074 slightly overlaps the right premaxilla showing that this specimen is distorted in a posterolateral direction. Surface texture of the premaxilla is slightly different on either side with the right premaxilla exhibiting a rougher surface texture than that of the left.



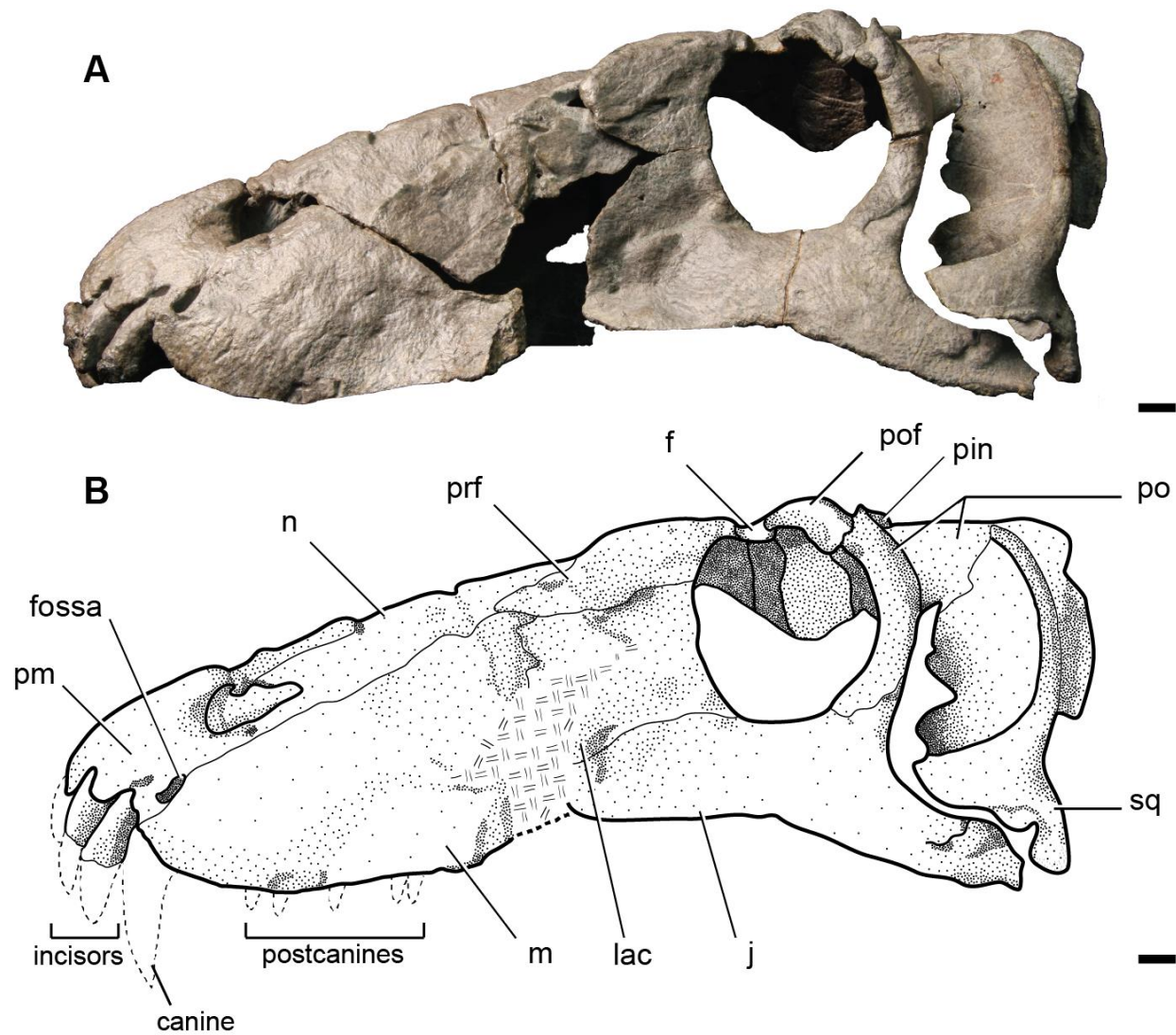


Figure 3.1: Photograph (A) and illustration (B) of BP/1/7074 in lateral view. Scale bars equal 1cm.

Housed in the left premaxilla are five upper incisors, and four are present in the right. Three incisors were removed from their alveolus prior to fossilisation and four preserve only their roots, still positioned in the alveolus.

The septomaxilla is a relatively thin and elongate bone visible on the right side of BP/1/7074 and has a short lateral exposure, contacting the premaxilla anteriorly.

Posteriorly, it is unclear how far the septomaxilla extends as in BP/1/7074 it appears to terminate within the margin of the external nares. In the smaller specimen of *Anteosaurus*, previously called *Micranteosaurus parvus* (SAM-PK-4323; Boonstra, 1954b), the limits of the septomaxilla are not known, and it is believed that the maxilla has a large overlap of the premaxilla (Boonstra, 1954a).

The holotype and only specimen *Australosyodon nyaphuli* has a clearer indication on the process of the septomaxilla, and in this specimen it forms the floor and the ventral portion of the posterior portion of the posterior side of the external naris (Rubidge, 1994). In other specimens of *Anteosaurus*, van den Heever and Rubidge (in prep) note that the septomaxilla also extends onto the lateral surface of the skull to meet the maxilla ventrally and posteriorly, and the nasals dorsally. The posterior process of the septomaxilla in other specimens of *Anteosaurus* forms a wedge between the nasal and maxilla (van den Heever and Rubidge, in prep). These features cannot be confirmed for specimen BP/1/7074.

The nasals are long and narrow, making up much of the dorsal skull with a midline nasal suture extending posteriorly, from the premaxilla up to the contact with the frontals at the frontoparietal boss (Figure 3.2). Anteriorly the nasals

contribute to the posterior border of the nares. In left lateral view the suture between the maxilla and the nasals is very distinct and runs horizontally across the lateral side of the skull, but the path of this suture is difficult to place with certainty on the right. The ventral surface of the nasals form a dome, with two ridges which extend posteriorly towards the prefrontals.

The maxilla is a relatively large bone, covering most of the lateral side of the snout. This bone has a long, dorsal sutural contact with the nasals, and has a pointed posterodorsal contact with the prefrontals. Sutural contact with the lacrimal is visible on the left lateral side, however this suture is not preserved in the lower portion, as the specimen is damaged in this area. Thus only the proximal portion of the lacrimal suture with the maxilla is preserved. Boonstra (1954a) states that the maxilla of *Anteosaurus* has a posterodorsal triangular tongue separating the jugal from the lacrimal. In BP/1/7074 the contact of the maxilla with the jugal is observed medially with a short vertical suture at the ventral margin of the skull, below the orbit. Anterior to the orbit the maxilla – jugal contact cannot be determined as this part of the skull is not preserved.

In palatal view the maxilla creates the posterior border of the maxillary fossa and forms the posterolateral margin of the alveolar of the fifth incisor. Both sides of the maxilla contains the canine in an extremely bulbous structure, which houses

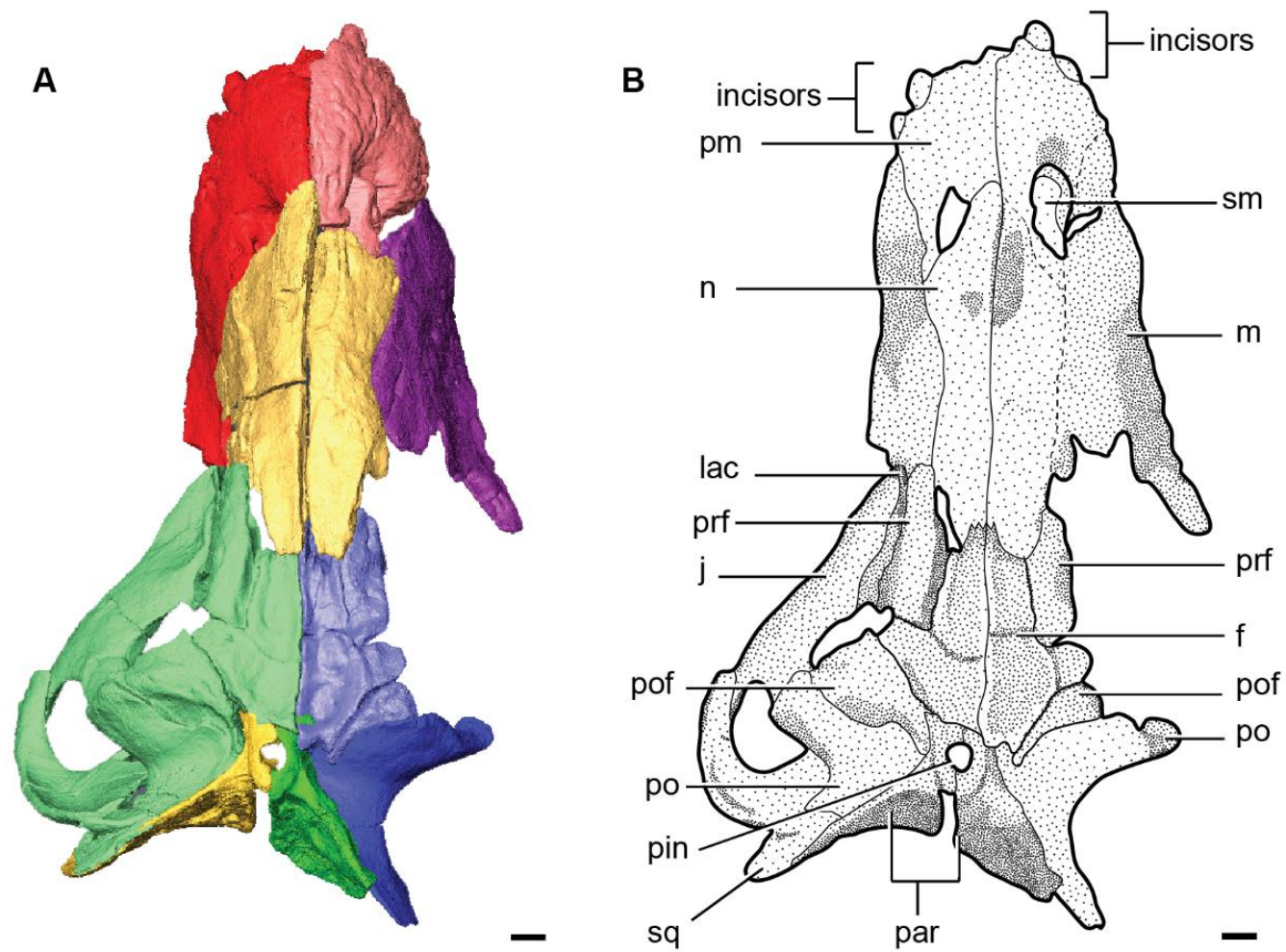


Figure 3.2: Reconstructed image (A) and illustration (B) of BP/1/7074 in dorsal view. Scale bars equal 1cm.

the root of the canines. This housing bulges medially and contain an oval fossa, at the middle of their structure (Figure 3.3).

Eight postcanine teeth are visible in the maxilla, the right maxilla houses three visible post canines, and the left has five. All of these teeth have been damaged and only the bases are visible. A large bulbous canine alveolus is present on the medial side of the maxilla (Figure 3.3). This globular structure slopes anteroventrally at approximately sixty degrees. The left boss preserves an erupting canine which is well preserved and only a small part of the crown has been damaged. The root and main corpus of the tooth is still embedded in the housing. On the right two canines erupt from this bulbous alveolus. The small, anteriorly positioned tooth is the replacement canine and is just above the alveolus. The more posteriorly positioned canine is the one being replaced, but is broken at the

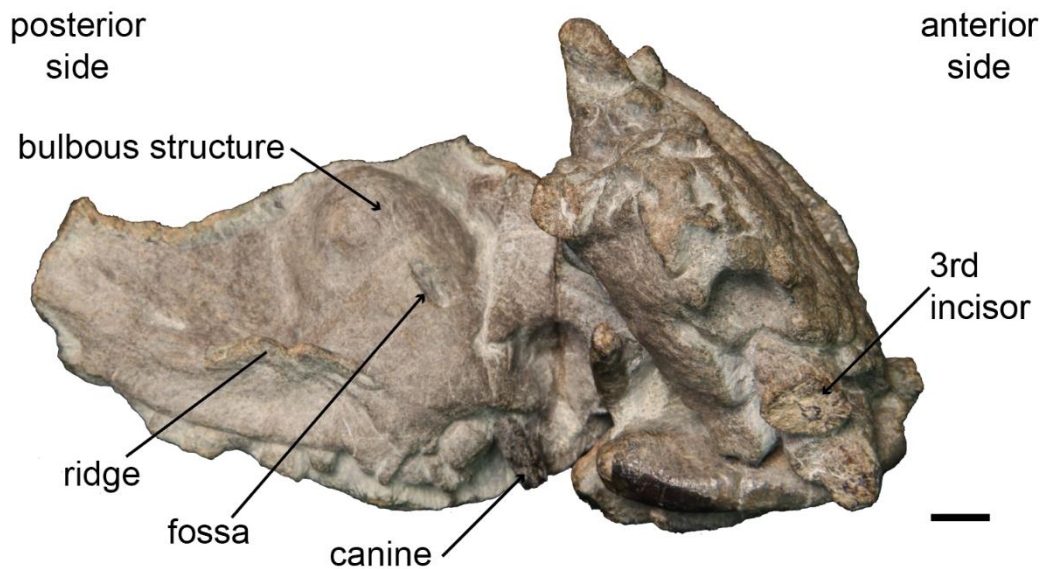


Figure 3.3: Photograph of left maxilla of BP/1/7074 in medial view. Scale bar equals 1cm.

crown. Medially the maxilla is thickest at the point of these two structures.

At the posterior side of the canine housing, and approximately at the mid-level of the bulbous structure, a thin shelf-like ridge extends posteriorly just above the level of the skull margin and postcanines. The dorsal edge of the ridge leads to a cup-like depression and the ventral shelf of this ridge accommodates the ventral anterior projection of the palatine bone of the palate. Thus contact of the maxilla with the palatine occurs posterior to the canine and anterior to the first postcanine, continuing posteriorly, to the posterior margin of the maxilla.

The anterior border of the left lacrimal is damaged and the lacrimal on the right side is not preserved. Boonstra (1954a) describes the lacrimal as being quadrilateral with a short sutural contact with the jugal, forming the anterior part of the orbital border. Posteriorly the lacrimal of BP/1/7074 forms the anterior border of the orbit, along with the prefrontal. In lateral view the lacrimal has a clear dorsal horizontally oriented sutural contact with the prefrontal, which occurs along a small ridge, similar to that described by Boonstra (1954a). This suture has a jagged appearance on the medial side of the skull (Figure 3.4). The anterior margin of the lacrimal contacts the maxilla and is visible in lateral view as a jagged suture below the anterior extent of the prefrontals, but only the dorsal-most portion is preserved. Posteroventrally the lacrimal meets the jugal with a long horizontal suture. On the medial side of the skull this is a very pronounced and winding suture which extends anteriorly from the inner ventral border of the orbit. The contact with the jugal along the aforementioned suture is at a raised step, and



on the medial side of the specimen, the lacrimal is positioned more medially and the jugal more laterally.

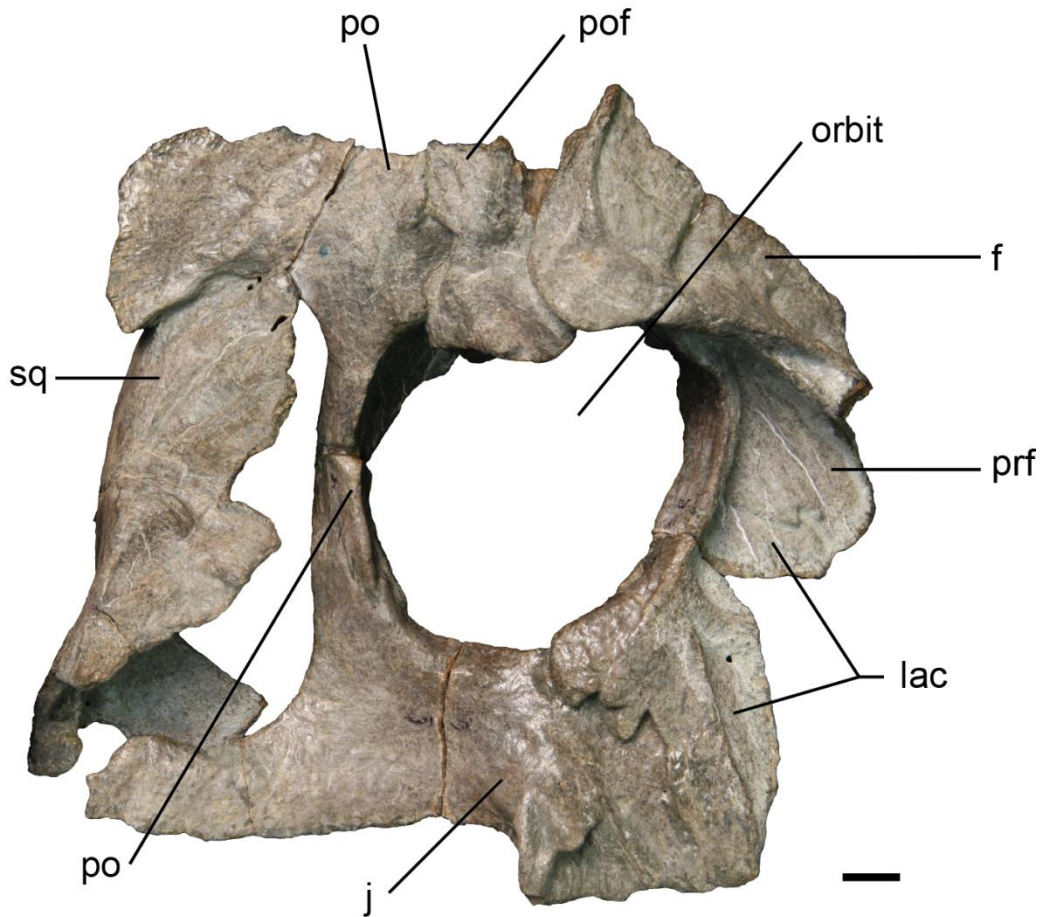


Figure 3.4: Photograph of left medial side of the skull of BP/1/7074 showing the bones surrounding the orbit. Scale bar equals 1cm.

The jugal is a large bone, forming the ventral and the posteroventral border of the orbit, where it meets the postorbital in a sutural contact which extends posterodorsally. Boonstra (1954a) considers that in *Anteosaurus* the jugal has an encroachment of the maxilla anteriorly, a feature not observed on BP/1/7074. In lateral view the jugal has its broadest exposure below the posterior orbital margin,

where it extends dorsally to contact the postorbital near the base of the postorbital bar. Posteriorly and ventral to the orbit, the jugal extends ventral to the squamosal, creating the ventral margin of the temporal fenestra. The outer surface of the jugal, along the ventral border of the temporal fenestra, is overlapped by the zygomatic process of the squamosal. The amount of this overlap, according to Boonstra (1954a) varies in different specimens. In lateral view, the contact between the lacrimal and the jugal is almost horizontal and occurs anterodorsally at the anteroventral margin of the orbit. The nature of maxillary contact with the jugal could not be determined as the skull is damaged in this region. The medial side of the jugal is a very smooth bone, which thickens posteriorly toward its contact with the postfrontal.

In lateral view the prefrontal is an elongate triangular bone with the apex pointing forward between the nasal and maxilla. Its ventral margin is almost horizontal and has a clear sutural contact with the lacrimal. In lateral view the prefrontal forms the anterodorsal part of the orbital border and contacts the nasals anteriorly. Dorsally, the prefrontal meets the frontal which extends laterally to the orbital margin with a distinctive and depressed suture which is visible on both sides of the skull of BP/1/7074. Dorsolaterally a thick rectangular portion of the frontal separates the prefrontal from the postfrontal. When viewing the prefrontal from the medial side, it is evident that the prefrontal is more thickened in this region than on its lateral side.

The paired frontals form the skull roof in the orbital region and exhibit a “tongue



like entry” into the dorsal border of the orbit (Boonstra, 1954a) which is fairly thin. In many *Anteosaurus* specimens thickening of the postorbital bar reduces the contribution of the frontal to the dorsal orbital margin and this is the situation in BP/1/7074. In contrast, the frontal of *Australosyodon nyaphuli* forms a large portion of the dorsal orbital border (Rubidge, 1994). The frontal is broadly triangular and in ventral view this triangular shape is more obvious with the apex facing anteriorly and the widest edges posteriorly (Figure 3.5).

In BP/1/7074 no pachyostosis is evident on the dorsal side of this bone, other than a slight thickening at the contact with the postfrontals at a sagittal suture, unlike the condition which is usually observed in large specimens of *Anteosaurus*. However, despite the relatively unpachyostosed appearance of the bone in BP/1/7074, in section it is evident that the frontals are dorsoventrally thickened. The anterior portion of the frontal is 1cm thick (dorsoventrally) compared to the posterior section which is 4,5cm. At its anterior end the frontal contacts the nasal with an interdigitated suture. Posteriorly the frontal meets the postfrontal along a ridge, which extends obliquely in a posteromedial direction from the dorsal orbital border toward the pineal opening. This is similar to the situation seen in *Australosyodon* (Rubidge, 1994).

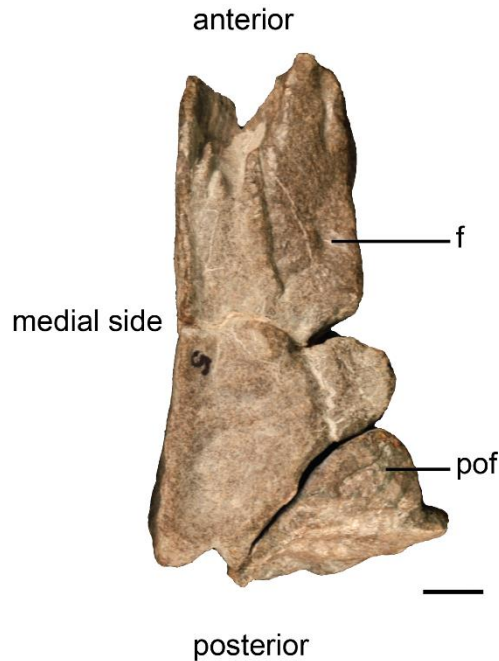


Figure 3.5: Photograph of right frontal and postfrontal of BP/1/7074 in dorsal view. Scale bar equals 1cm.

Positioned posterior to the frontal, the postfrontal is a small triangular bone, which together with the frontal and postorbital, makes up the posterodorsal orbital border where the longest side is present and is thickened to form a boss which overhangs the posterodorsal border of the orbit. From here the postfrontal tapers to a point between the postorbital laterally and the parietal on the medial side. Posteriorly, the postfrontal has a depression on its dorsal surface anterior to its contact with the postorbital, which has a slight sigmoidal suture and overhang. Boonstra (1954a: 113) states that “In the forms where the thickening of the frontal is not very great the postfrontal forms part of the dorsal outline of the skull when observed in lateral view; in the other forms it nearly reaches the dorsal edge or lies well below it.” Boonstra (1954a) also noted that when well-developed the

postfrontal intrudes onto the frontal and overlaps the postorbital on the postorbital bar, limiting the contribution of the frontal to the dorsal margin of the orbit. This may cause variation in the position of the postfrontal-postorbital suture.

The postorbital is roughly triangular and both left and right postorbitals are preserved in BP/1/7074. They present two distinctive surfaces; the lateral surface forms part of the postorbital bar, and the dorsal surface part of the intertemporal region. The postorbital contacts the jugal ventrally. Dorsally, the postorbital is greatly thickened, and is at its thickest at the posterodorsal margin of the orbit. The postorbitals overlap the posterodorsal portion of the postfrontals and this leaves a trough-like sutural contact between the two bones which is extremely evident in dorsal view. Boonstra (1954a) notes that the ventral extent of pachyostosis in the postfrontal determines the degree at which it overlaps the postorbital. The case of BP/1/7074 contradicts this observation and the postfrontal does not overlap the postorbital. Dorsomedially the postorbital forms the thin pane of bone which forms the lateral face of the intertemporal region. When viewing the postorbital from the medial side, a deep foramen is present on the dorsal side behind the dorsolateral portion of the parietal.

When viewing the bones which comprise the margins of the orbit from the medial side of specimen BP/1/7074, there is a marked difference in thickness. The ventral margins, encompassing the jugal and lacrimal, are extremely thin, whereas the lateral margins, being made up of the lacrimal (anteriorly) and the postorbital (posteriorly) are considerably thicker. The orbit border becomes exceptionally

thick (approximately five times thicker) at its medial roof which is created by the frontal, postfrontal and postorbital bones and make up the braincase. The thickest part of the orbital border is formed by the postorbital bone, which is not only thicker at this point than any adjacent lying bones, but also sits slightly lower within the orbital border.

The squamosal is a large, thin bone comprising the posterior and ventral borders of the lateral temporal fenestra. Along the posterior border of the lateral temporal fenestra, the squamosal is noticeably thicker. The left squamosal of BP/1/7074 is well preserved whereas the right is missing part of its middle portion.

Anterodorsally the squamosal meets the postorbital, medially it contacts the parietal. This smooth, curved bone curves in a lateral direction before meeting the jugal anteroventrally. Posteromedially, it is covered by the tabular on the occipital surface. Between the zygomatic process and the inner facing of temporal fenestra, a small notch is created which houses the quadrate.

Both the left and right parietal bones are preserved, and were separated from the surrounding bones during preparation. Each parietal is relatively small and quite thick. On the skull roof the parietal fits neatly behind the curved posterior part of the postorbitals and has an anterior sutural contact with the frontal which is situated along a transverse ridge. The pineal foramen which is slightly ovoid, is situated on a large boss at the end of long tubular prominence (Figure 3.6).

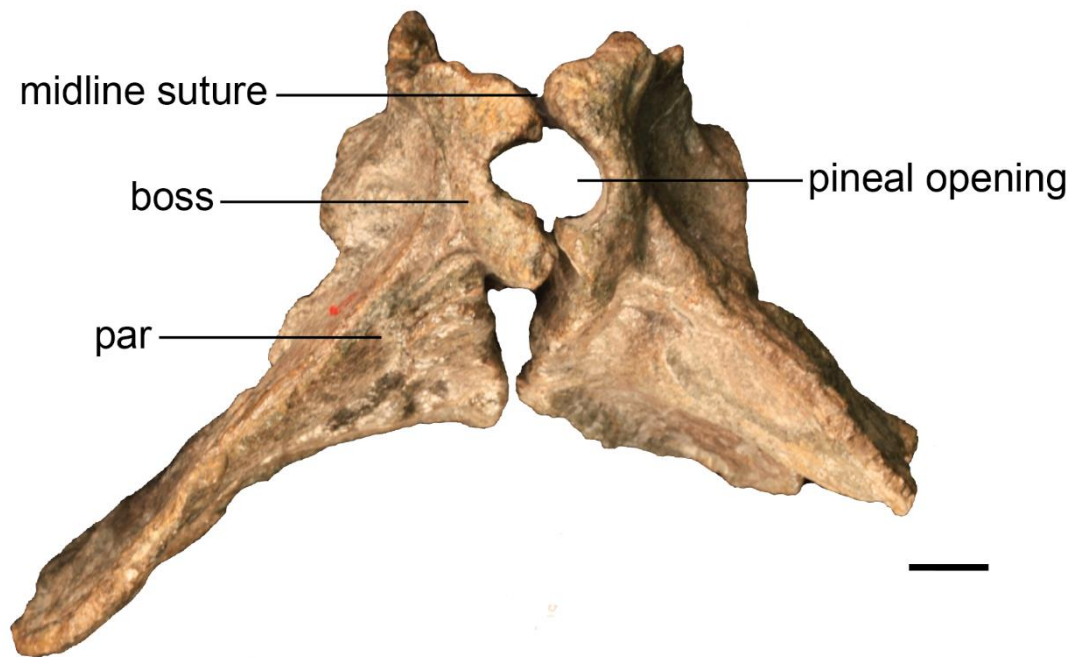


Figure 3.6: Dorsal view of left and right parietal, and pineal opening of BP/1/7074. Scale bar equals 1cm.

In posterior view, where each parietal bone meets the other, a longitudinal median ridge protrudes from the dorsal edge to beneath the overlapping interparietal and forms the posterior border of the pineal foramen. A posterior view of the parietal bone exposes a short longitudinal sutural contact with the interparietal which occurs laterally. At this meeting of the parietal and interparietal, a deep foramen is present on the right parietal bone, mirrored by a slightly shallower foramen on the left parietal bone. Anteriorly the parietal bone has a small midline anterior projection with a vertical ridge which extends between the frontals and the medial sides of the postfrontal and postorbital bones.

### 3.2.3 Palate

The palate of BP/1/7074 is well preserved, however elements on the left side are better preserved than those on the right. The premaxilla is complete but portions of the right vomer and palatine are missing. The pterygoids and basisphenoid are well preserved.

In ventral view the premaxilla is relatively small and forms the anterior part of the skull (Figure 3.7). Posterolaterally it contacts the maxilla with a clear oblique suture anterior to the canine and posterior to the fifth incisor. Just posterior to the medial side of the fifth incisor a maxillary fossa is present and the suture between the premaxilla and maxilla extends through this fossa. Posteromedially the premaxilla has a short contact with the vomer. The maxillary fossa receives the crown of the lower canine when the jaws occlude, and is relatively deep. Medially as the maxillary fossa deepens, the premaxilla – maxilla suture runs directly through it, thus the maxillary fossa occurs between the premaxilla and maxilla bones. This is different from the suture described for *Australosyodon* (Rubidge, 1994) where the maxilla – premaxilla suture is immediately posterior to the maxillary fossa in the upper jaw. The maxilla – premaxilla condition is thus similar to *Syodon*, *Doliosauriscus* and *Titanophoneus* (Orlov, 1958) which all have a suture which transverses the maxillary fossa of the upper jaw. The maxillary suture extends posteriorly down the flanks of the specimen. Anteromedially the premaxilla creates the anteromedial border of the internal naris.

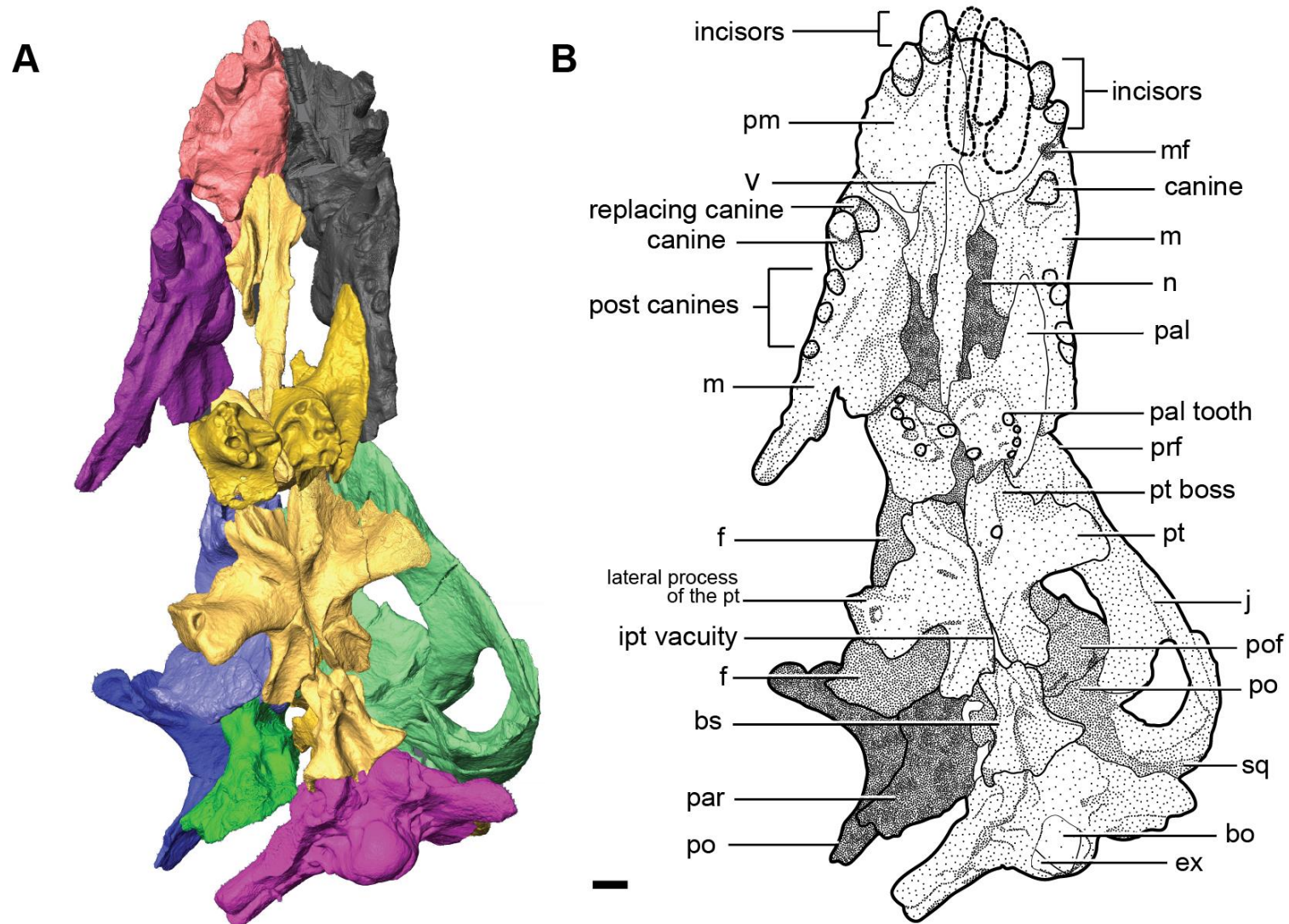


Figure 3.7: Reconstructed image (A) and illustration (B) of BP/1/7074 in ventral view. Scale bar equals 1cm.

The paired vomers are narrow, elongate bones. Anteriorly the vomer is rounded in cross section, extending posteriorly towards the palatine where it becomes flattened and broadened medially. A midline suture is present between the paired vomers. Posteriorly the vomer presents a medial ridge which extends approximately half the length of the vomer, terminating before the level of the palatine boss. The lateral edges of the vomer are folded medially in ventral view and resemble that of *Syodon*. The vomer continues posteriorly above the raised palatine bosses as a pointed, hollow triangular bulbous structure which is positioned on the dorsal side of the pterygoid and palatine bosses (Figure 3.8).

An anterolateral projection of the palatine overlies the posteroventral side of the maxilla and is not preserved on the right side. Posteriorly the palatine forms a prominent ventrally protruding dentigerous boss. The lateral margins of the palatine bosses each have five small conical teeth which are arranged in a concentric semicircular row. Posteriorly the palatine boss of the palatine meets the pterygoid with a zig-zag sutural contact. At this intersection between the palatine boss and anterior ramus of the pterygoid, one conical tooth is present on the left medial pterygoid boss. No teeth are present on the right pterygoid boss.

The ectopterygoid is not preserved and probably became disarticulated prior to fossilization. This bone is usually positioned anteromedially to the lateral pterygoid process. Boonstra (1954a) states that the ectopterygoid meets the palatine, maxilla and jugal, forming the upper part of the lateral and anterior face of the lateral pterygoid process. In *Syodon* and *Titanophoneus*, the ectopterygoid



contacts the jugal posteriorly and Boonstra (1954b) believed this to be the case for *Anteosaurus* as well.

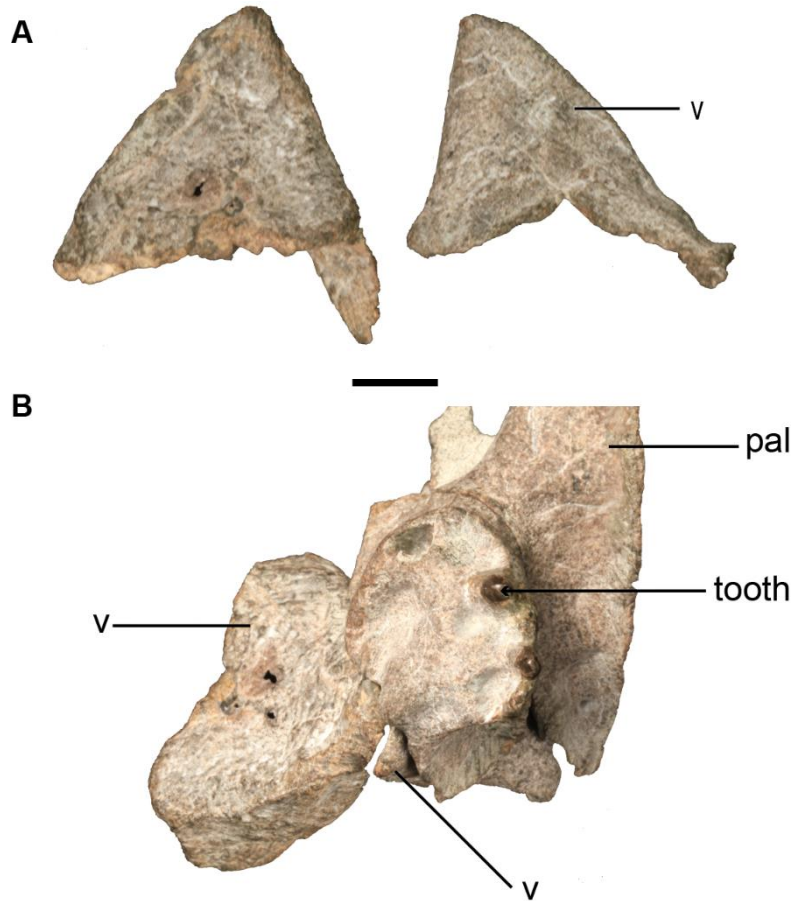


Figure 3.8: (A) Photograph of posterior projection of the left and right vomer of BP/1/7074 which continues under the palatine in a triangular form, in lateral view; (B) photograph of position of the posterior projection of the vomer with relationship to the palatine and palatine boss. Scale bar equals 1cm.

The pterygoid is a large bone exhibiting three rami (Figure 3.9). Anteriorly, the anterior ramus of the pterygoid contacts the palatine boss and anterolaterally has a small contact with the palatine. The anterior ramus has one small conical tooth present on the left side. The transverse flange of the pterygoid extends laterally, and produces a ridge-like structure continuing to the lateral border of the pterygoid. This is where the pterygoid is thickest and forms a bulge in the middle of the bone. No teeth are evident on the lateral ramus of the pterygoid. The basicranial ramus of the pterygoid curves posteriorly, contacting the basisphenoid. A parasagittal ridge is present on the basicranial ramus of the pterygoid that extends from the transverse processes to the contact with the basisphenoid. Medially, the basicranial ramus has a trough which lies between the process of the lateral ramus and the posterior end of the basicranial ramus.

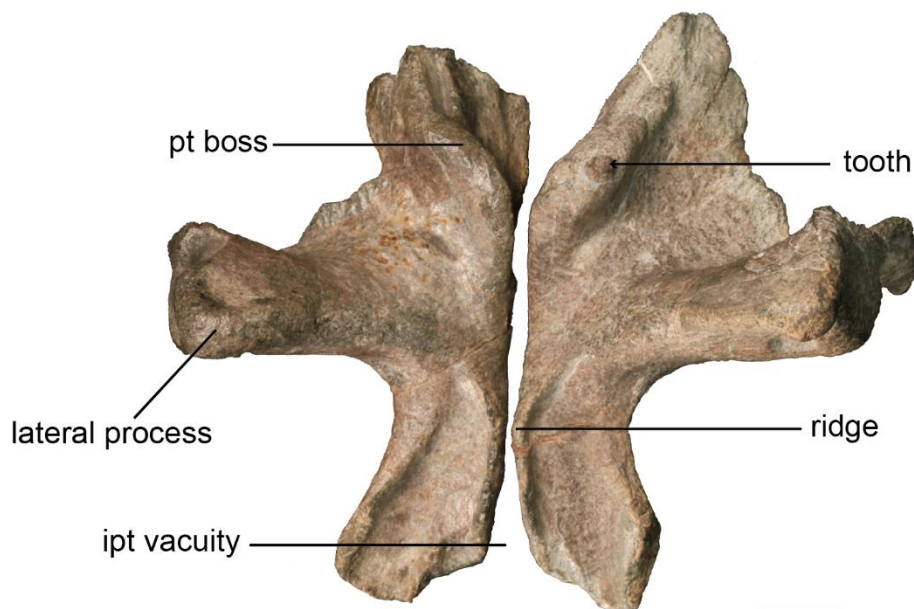


Figure 3.9: Photograph of left and right pterygoids of BP/1/7074 in ventral view.  
Scale bar equals 1cm.

The basisphenoid is a complex bone, possessing many ridges and facets. In ventral view it contacts the basicranial ramus of the pterygoids anteriorly, and widens posteriorly where it meets the basioccipital. Ventrally the basisphenoid has a deep trough which extends from approximately the midline of the corpus to the posterior border of the corpus. Immediately anterior to this trough, a midline crest is present with a lateral fossa on each side. The midline crest does not extend as far as the anterior margin of the basisphenoid. In lateral view, the dorsal side of the basisphenoid has a more prominent crest, which is rectangular. This crest occupies the middle of the corpus, and terminates posteriorly before a shallow trough. The shallow trough, continuing onto the basicranium, finally terminates on the anterior side, at the ventral margin of the foramen magnum. A posterior view of the basisphenoid shows a lateral articulation which meets two corresponding condyles on the basioccipital.

### **3.2.4 Occiput**

The occiput (Figure 3.10) is well preserved missing only a portion of the right tabular, parietal and squamosal. The supraoccipital, opisthotic and tabulars are fused together. The foramen magnum is large and triangular.

In occipital view, the interparietal is best preserved on the left, and a small portion is still apparent on the right side. The parietal extends posteriorly onto the dorsal occipital surface, and the interparietal overlaps it on the posterior side. Ventrally the interparietal contacts the supraoccipital along a horizontally curved suture.

The interparietal becomes thicker at its base, before contacting the supraoccipital, and is considerably thin at the point of overlapping the parietal bones.

The tabulars are thin, smooth, semilunate curved bones, extending laterally in occipital view. A larger portion of the left tabular is preserved compared to that of the right. The ventral portions of the tabulars are not preserved on the right side.

The tabulars partly cover the posterior portion of the postorbital, parietal and squamosal bones. A ridge like suture contacts the tabulars with the interparietal. The interparietal is slightly raised and overlaps a small portion of the tabulars on the medial side.

The supraoccipital is a transversely broad bone, situated ventral to both the interparietal and tabular bones and forms the dorsal border of the foramen magnum. Posteriorly, the suture between the interparietal and supraoccipital is distinct, however contact with the tabular is unclear. Ventrally the supraoccipital is completely fused to the opisthotic and it is difficult to make out sutures, even though this specimen is a juvenile.

The opisthotic is a large bone making up the posteroventral part of the occipital region. It forms a concave surface which deepens toward the foramen magnum. The paroccipital process of the opisthotic is more apparent on the right side of the specimen, contacting the supraoccipital dorsally, the basioccipital ventromedially, and the tabular dorsolaterally.

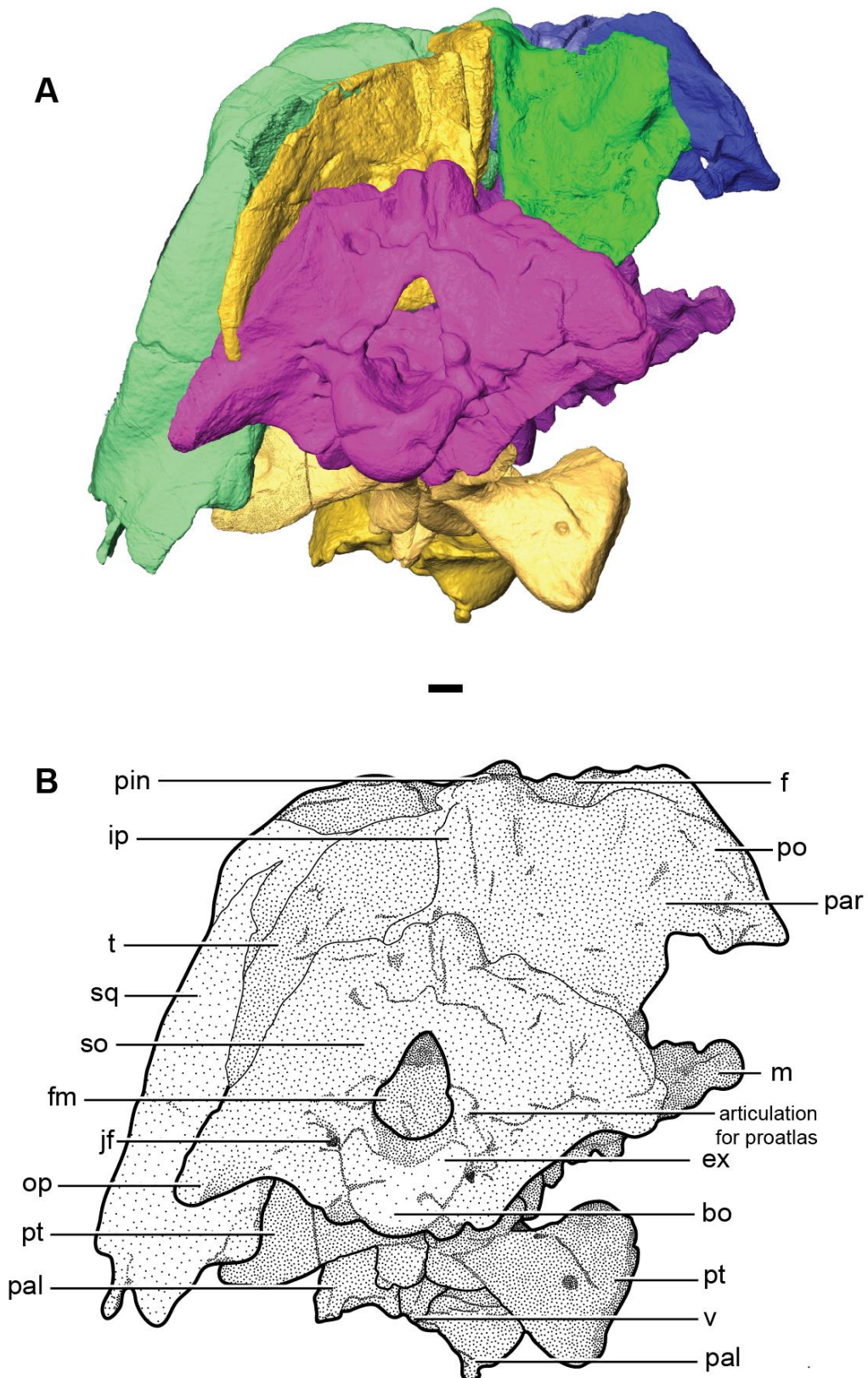


Figure 3.10: Reconstructed image (A) and illustration (B) of BP/1/7074 in occipital view. Scale bar equals 1cm.

Paired exoccipitals which are triangular and relatively small, form the lateroventral and ventral margin of the foramen magnum. Ventrally they meet the basioccipital and protrude from the ventral and lower lateral margins of the foramen magnum and continue posteriorly onto the occipital condyle. A jugular foramen is present on each side of the occipital condyle, just below the dorsolateral suture of the exoccipitals. Medial to the jugular foramen is a fossa of comparable size. Above the exoccipitals, at the ventrolateral border of the foramen magnum, is small oval protrusion which articulates with the proatlas.

The basioccipital is smooth and rounded, wedging between the two posteriorly projecting exoccipitals and creating the ventral portion of the occipital condyle. On the occipital surface the basioccipital meets the opisthotic dorsolaterally, and on the palate it is in contact with the basisphenoid anteroventrally.

Both quadrates are preserved as separate disarticulated bones (Figure 3.11). In most adult *Anteosaurus* specimens, the quadrate is preserved in articulation with the squamosal and is not always visible. In BP/1/7074 it is evident that, the quadrate is a broad spoon-shaped bone and in lateral view has a convex profile. The right quadrate and quadratojugal is more rounded anteriorly. The dorsal surface of the quadrate is rounded and along the ventral side it has an “S” shaped ventral margin comprising two articulatory condyles. The medial trochlear condyle is slightly larger than the lateral trochlear condyle. The contact facet is convex and a small quadrate foramen is present ventrolaterally. A fairly deep lateral notch is present. In life the dorsal plate of the quadrate would have

articulated with the squamosal and the ventral condyles of the quadrate would have articulated with the quadrate ramus of the pterygoid. The right quadrate has a thin ridge which extends anteriorly towards the lateral trochlear condyle.

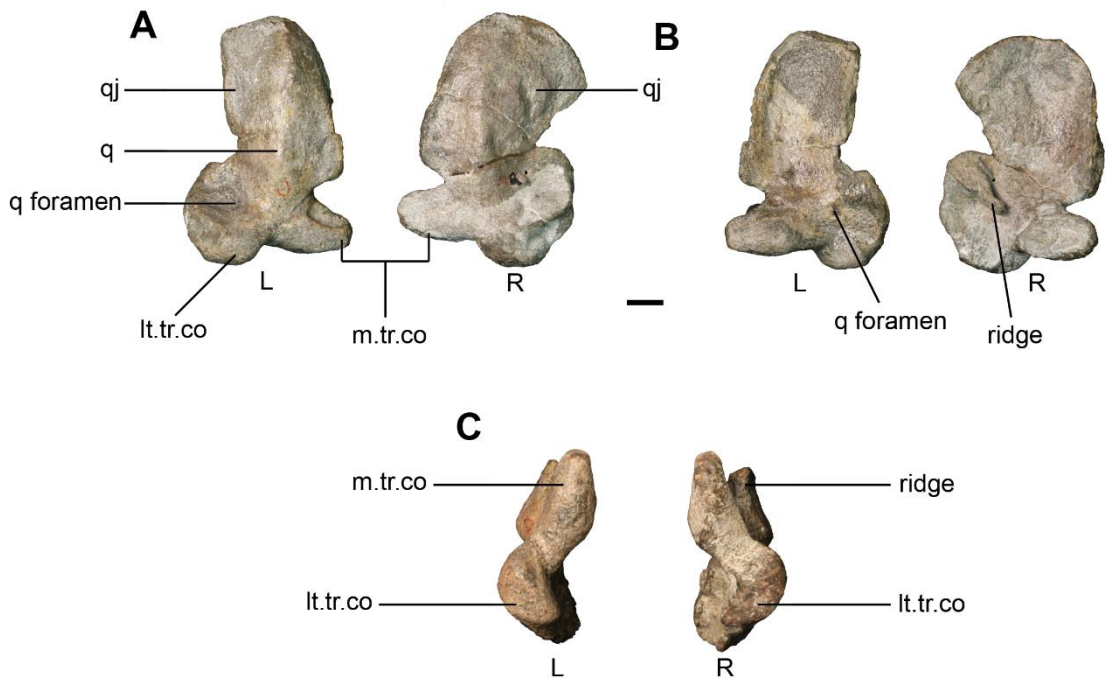


Figure 3.11: Photograph of left and right quadrate bones of BP/1/7074 in (A) anterior view; (B) posterior view; and (C) ventral view. Scale bar equals 1cm.

### 3.2.5 Lower Jaw

Only a small anterior portion of the dentary of BP/1/7074 is preserved and one incisor and a canine are evident (Figure 3.12). Only the base of the canine is present which is oval in cross section and features longitudinal striations which



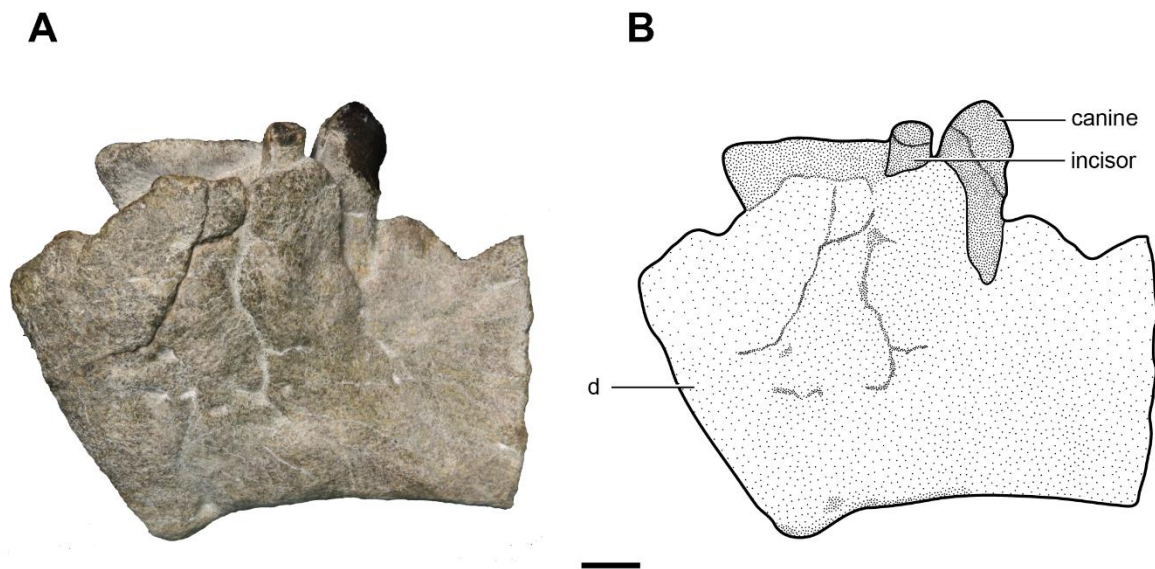


Figure 3.12: Photograph (A) and illustration (B) of left dentary of BP/1/7074 in lateral view. Scale bar equals 1cm.

cover the entire surface. No serrations are present on the lower portion of the canine. It is evident that the root is large as this causes a bulge on the medial side of the mandible. The preserved incisor is also oval in cross section and does not possess a heel. The incisor is oval and slight curved posteriorly. On the medial side of the left mandible a broad trough separates the dentary from the splenial. Much of the posterior dentary and splenial is absent and thus the nature of this suture is unknown.

Only a very small section of the angular is preserved, separated from the other elements of the lower jaw. The bone is not well preserved and has been weathered extensively. The angular exhibits a rough surface with a small rounded disk-shaped protuberance.



### 3.2.6 Dentition

As noted by Boonstra (1962) the crowns of the teeth are seldom preserved in *Anteosaurus*. Weathering erodes the crowns away, and in some cases the skulls lay exposed before being covered by sediment and fossilized, leading to the teeth either falling out or the crowns being broken off. Most anteosaurids have the crowns broken off at the level of the alveolar border during fossilization or later on during weathering of the rocks in which they lie. Boonstra (1962) believed that the crowns of the anteosaurids were broken off at the level of the alveolar more frequently than those of any other infra-order of Dinocephalia, and attributed this to the difference of implantation as well as the mode of replacement of the teeth of the different infra-orders.

The premaxilla of BP/1/7074 has five incisors on the left and four on the right. Three of these incisors still preserve much of their crowns (Figure 3.13A). The incisors are oval and long, curving slightly posteriorly. No heels are present on the incisors. Three of the nine upper incisors became displaced from the alveolus prior to fossilization and were preserved at the tip of the snout. The incisors have a long and curved conical root which is oval in cross section. Along the surface of the incisors, longitudinal striations run the entire length of the teeth. In the left dentary only one incisor and a canine are preserved.

The left upper canine, which was just erupting at the time of death, is visible with only the crown protruding. On the right side however, both the canine and the

replacement canine are preserved (Figure 3.13B), and the replacement canine is positioned anterior to the existing canine. The upper canine is more robust than the incisors and is longitudinally oval in general shape. The lower canine is slightly smaller but has been broken off just above the alveolus so that most of the crown is not preserved.

A total of eight postcanines are preserved (Figure 3.13C). The left side of the skull houses five of these postcanines whereas the right has only three. The postcanine crowns are mostly damaged although one crown is preserved and has a sharp edge. The first upper-right postcanine of the maxilla is the best preserved. The postcanines are oval and when viewing the left upper jaw, it is evident that the postcanines become reduced in size in a posterior direction. No postcanines are preserved on the dentary and only one empty alveolus is evident. The dentary is damaged about three centimetres posterior to the canine.

### **3.2.7 Cervical Vertebrae**

Along with the atlas-axis complex, two post-axial cervical vertebrae have been preserved with the skull of BP/1/7074. The atlas centrum is a free element from the complex. One triangular intercentrum is preserved as a free element.

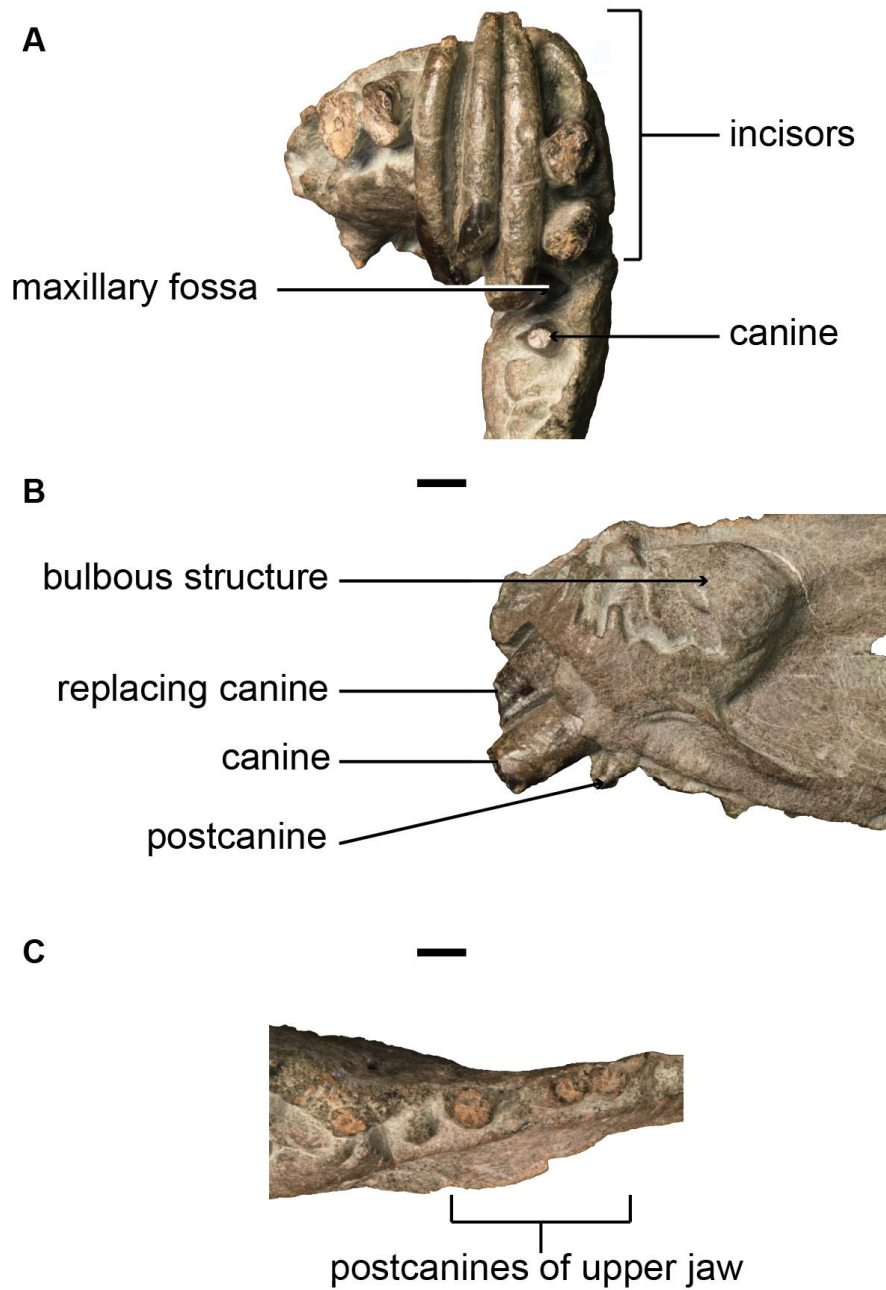


Figure 3.13: Dentition of BP/1/7074: (A) Photograph of incisors in ventral view; (B) photograph of canine and replacing canine of the right maxilla in medial view; (C) photograph of postcanines of the left maxilla in ventral view. Scale bars equal 1cm.

The flat and triangular proatlas is preserved and attaches at the ventrolateral border of the foramen magnum, where an oval protrusion exists just above the exoccipital and occipital condyle.

In dorsal view the atlas centrum has a broad trough which forms the floor of the neural canal (Figure 3.14). Dorsolaterally a pair of flat oval facets are positioned above the neural canal. Posterior to the dorsoventrally flattened facets, the bone slopes posteroventrally to the posterior margin of the atlas centrum. Anteriorly a slight convex bulge occurs and terminates at the anteroventral margin. Ventrally, it takes on a rectangular shape which tapers slightly posteriorly. In posterior view, a concave articulating facet is present which has a deep point, and meets the middle of the dorsal neural arch.

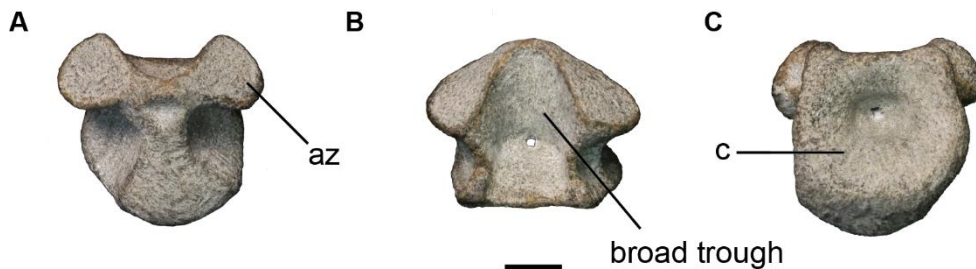


Figure 3.14: Photograph of the atlas centrum of BP/1/7074 in: (A) anterior view; (B) dorsal view; and (C) posterior view. Scale bar equals 1cm.

The axis resembles the two post-axial cervical vertebrae in morphology aside from the neural spine being much shorter in height and broader in lateral view as well as lacking a posterior projecting transverse process of the neural arch (Figure 3.15). In anterior view the axis has a thickened triangular neural spine. Below the

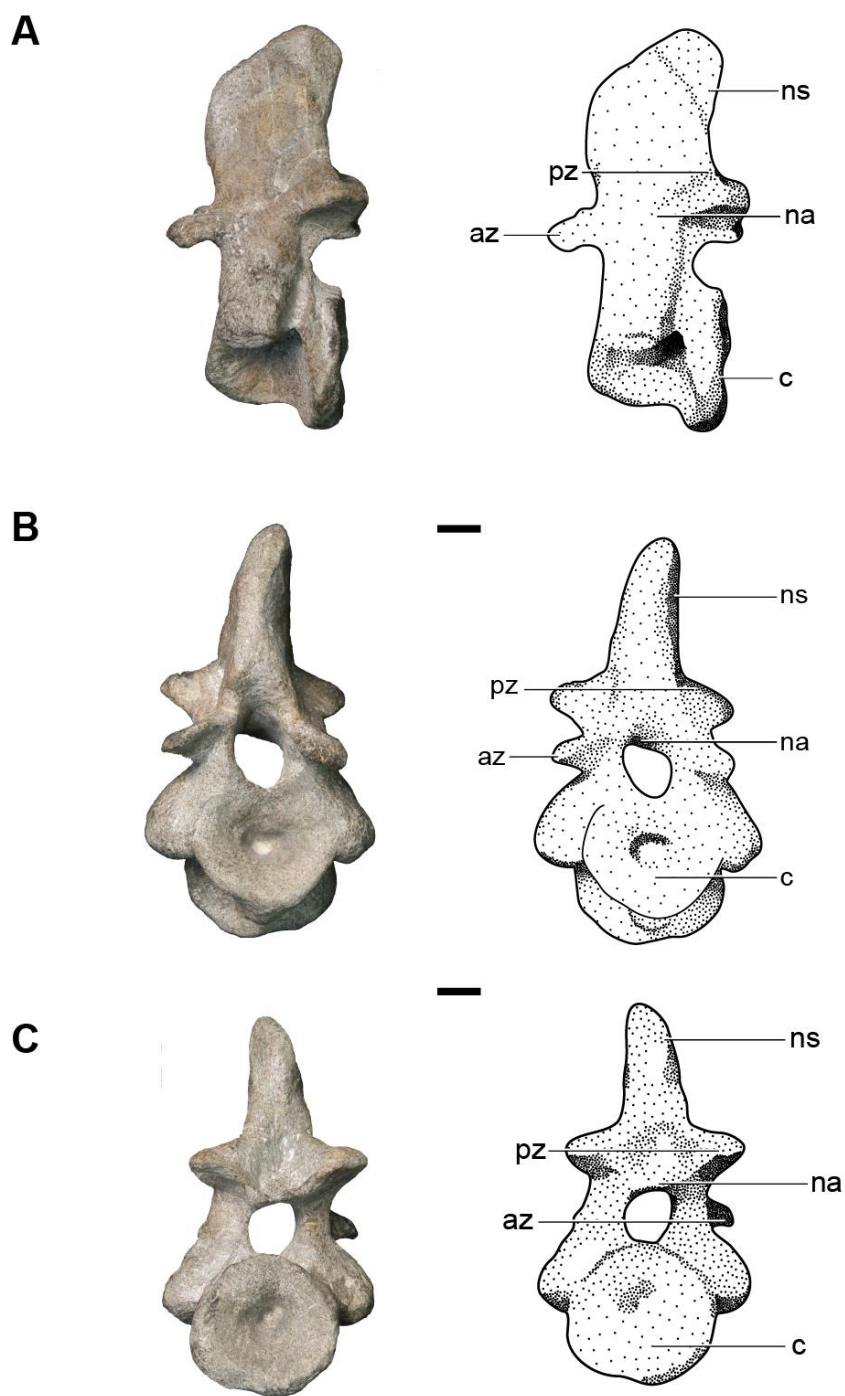


Figure 3.15: Photograph and illustration of the axis of BP/1/7074 in: (A) lateral view; (B) anterior view; (C) posterior view. Scale bars equals 1cm.

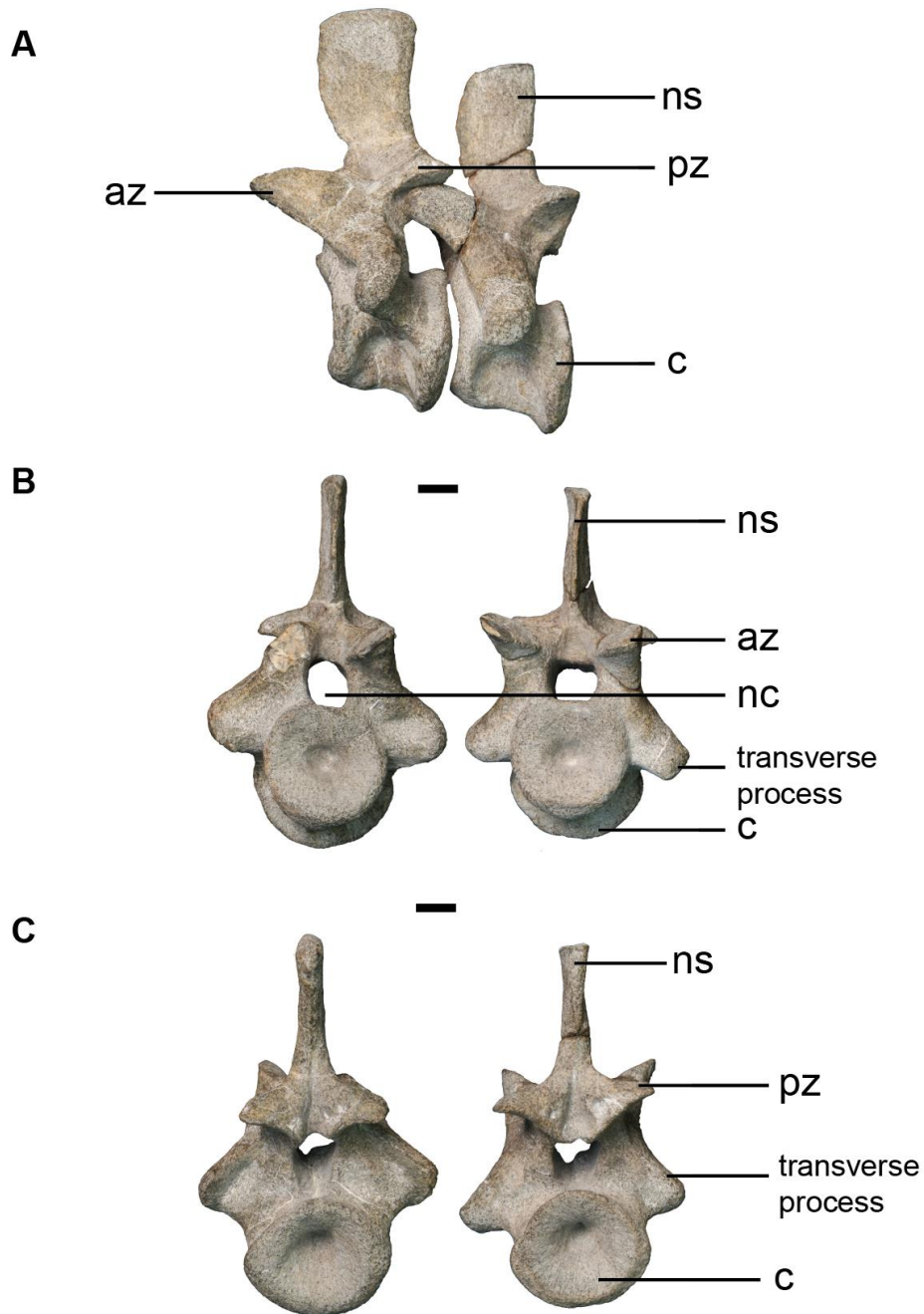


Figure 3.16: Photograph of the third and fourth cervical vertebra of BP/1/7074 in (A) lateral view; (B) anterior view; (C) posterior view. Scale bars equal 1cm.

neural spine, at the lateral margins of the neural arch, the anteriorly directed zygapophysis are relatively short. The anterior centrum is similar to that of the atlas centrum. Lateral to the centrum, in anterior view, a transverse process is present, however this process extends further ventrally compared to that of the process of the post-axial vertebra which extends more laterally. In posterior view, the centrum is round with a deep articulating facet. Ventral to the neural spine, the posterior zygapophysis ventrally positioned facets which lie laterally to the anterior margin of the neural arch. Between the posterior zygapophyses a deep diamond shaped hollow is present.

The remaining cervical vertebrae, are similar in size and shape (Figure 3.16). The third cervical vertebra has a taller neural spine compared to that of the fourth cervical vertebra. In anterior view, the centrum is round with an articulating facet. Dorsal to the articulating facet, the neural arch is an oval shape. The anterior zygapophyses extend a greater length compared to that of the axis, and have dorsomedially facing facets.

### **3.3 Microfocus X-Ray Computer Tomography (CT) Scanning and 3-D Reconstruction**

As most of the elements of BP/1/7074 are preserved in some way but have been subjected to some distortion, and most of the right side of the skull has been damaged, it was decided that to accurately reconstruct the skull of this juvenile *Anteosaurus* using digital scanning techniques. Digital techniques were used to position each bone in its place and build up a full reconstruction of the specimen. Because much of the right side of BP/1/7074 is damaged the reconstruction was accomplished by mirroring parts from the left side of the skull. Three incisors were manually segmented from the 3-D scan of BP/1/7074 and replaced more accurately after the reconstruction of the snout was completed.

The right premaxilla, although mostly intact, was removed from the digital reconstruction and mirrored from the left premaxilla (Figure 3.17). This afforded a more accurate reconstruction of the premaxilla as well as creating a straight connection for the vomers to contact the premaxilla. The nasal was left untouched for the reconstruction, as most of this bone is preserved. The right maxilla of BP/1/7074 is preserved, but does not fit well with the right premaxilla and the nasal in the specimen. Accordingly the right maxilla was reconstructed from the more accurate left maxilla. Apart from the right frontal, the right side of BP/1/7074, including the jugal, lacrimal, prefrontal, postfrontal, postorbital and squamosal, is not as well preserved as that of the left. Therefore these six elements were reconstructed from the left side of the skull and joined up with them. This resulted in an almost complete reconstruction of the right side of the skull,



incisors

pm

n

pof

par

sq

pin

62

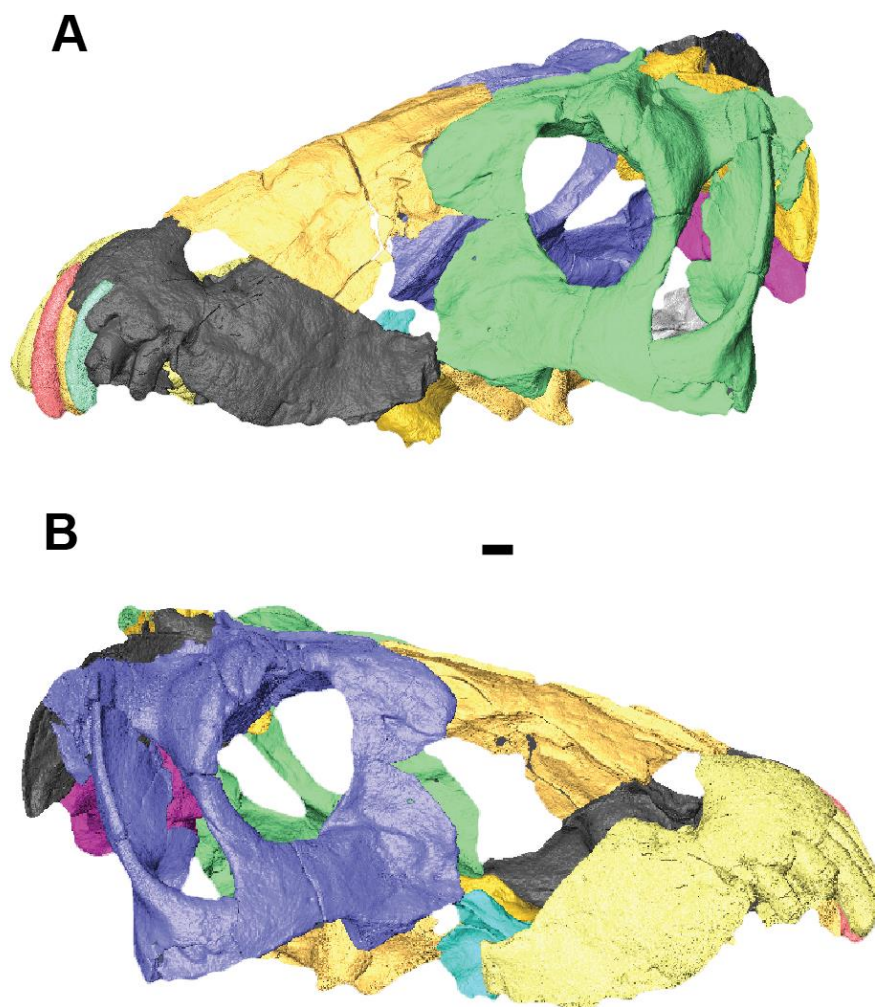


Figure 3.18: 3-D reconstruction of BP/1/7074 in (A) left lateral view and (B) right lateral view. Scale bar equals 1cm.

On the occiput of BP/1/7074 it was necessary to reconstruct only the right parietal from the left side, as the supraoccipital, basioccipital and exoccipitals are well preserved and were not separated during mechanical preparation (Figure 3.19). The right parietal was reconstructed from the left and then paired with the left parietal, and then fitted with the tabulars and supraoccipital.

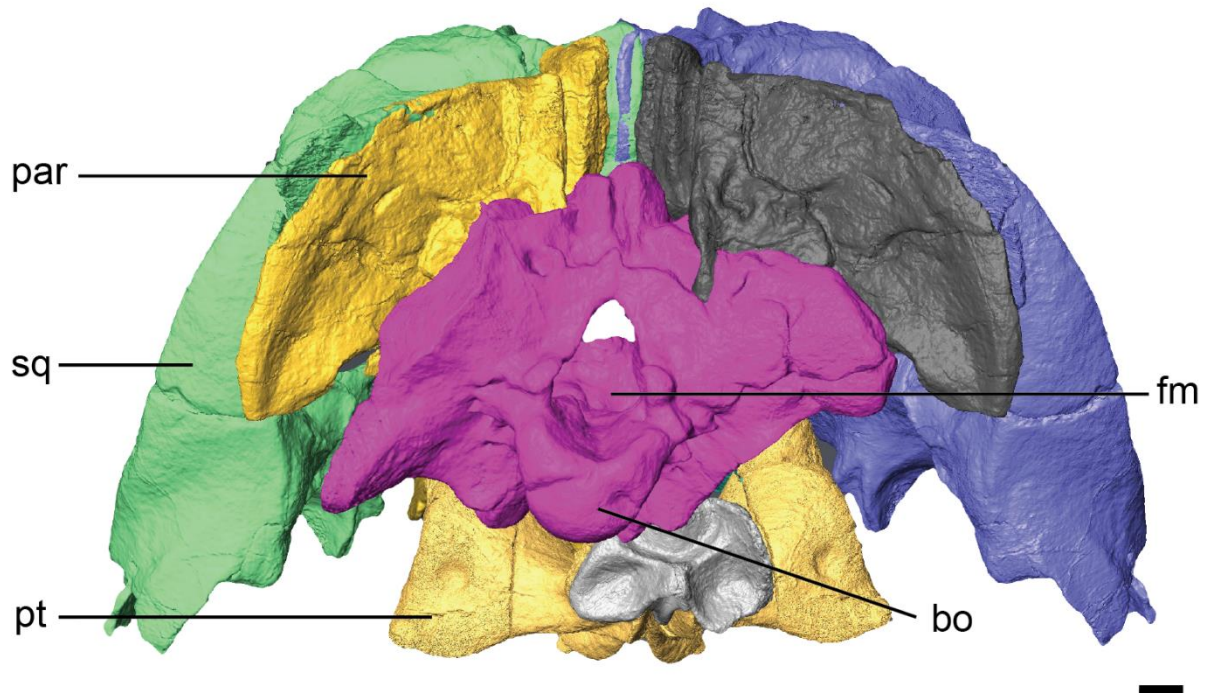


Figure 3.19: 3-D reconstruction of BP/1/7074 in occipital view. Scale bar equals 1cm.

In the palate, similarly to the skull roof, some elements were not as well preserved on the right side compared to that of the left. The right vomer was reconstructed from the left and then paired together (Figure 3.20). The vomers then fitted neatly in an oval groove, preserved in the posterior section of the premaxilla and in the reconstruction are not distorted as they are in life. When reconstructed the vomers are morphologically similar to that of *Syodon* whereby the lateral edges of the vomer have been curved over to almost meet each other medially.

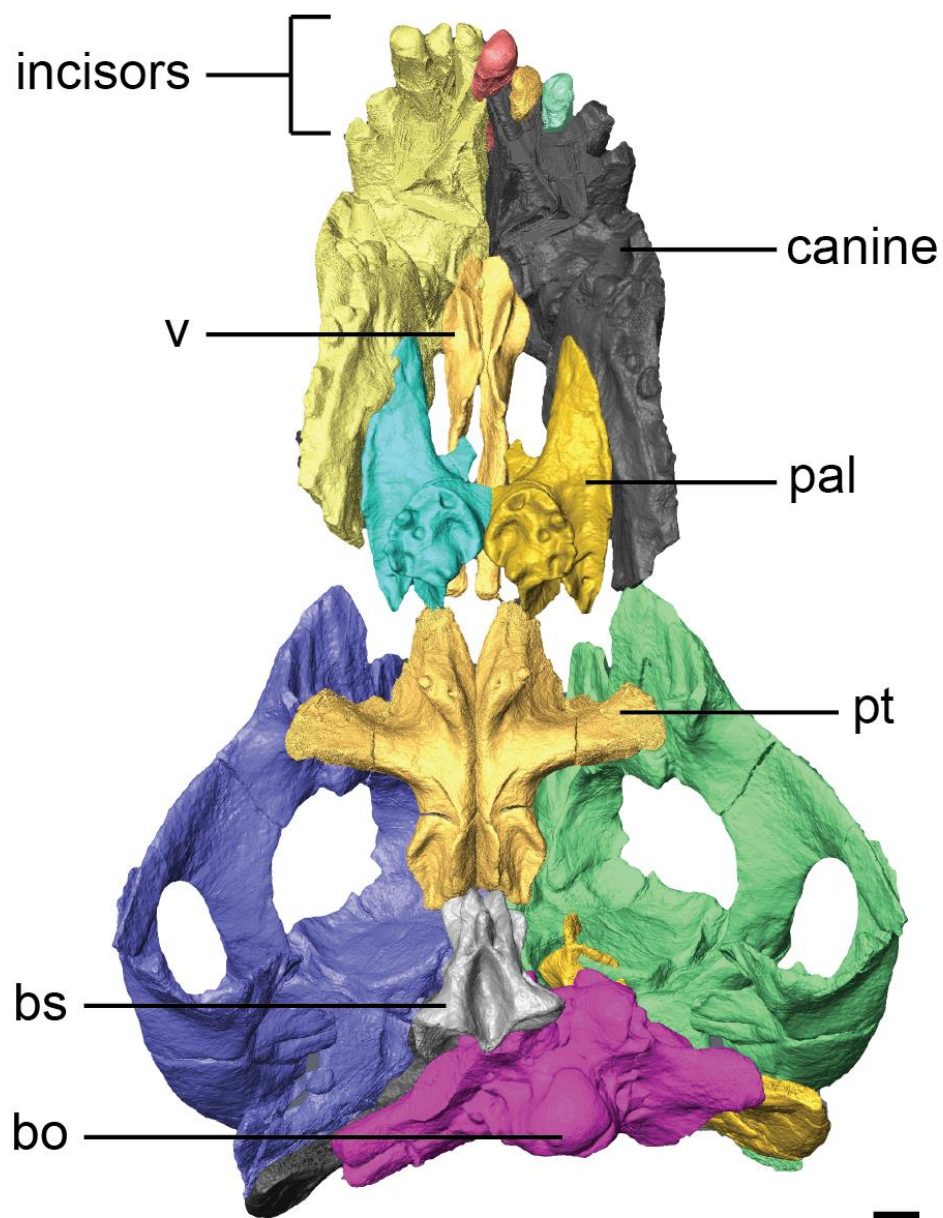


Figure 3.20: 3-D reconstruction of BP/1/7074 in ventral view. Scale bar equals 1cm.



The right palatine is not as well preserved as that of the left, as only the right palatine boss is preserved, without the anterior projection of the palatine which contacts the maxilla anterolaterally. This element was thus mirrored from the left, complete palatine and were fitted with the posterior end of the vomers. The vomers were straightened out slightly, relieving the anteroposterior deformation of the palate. The same applied for the pterygoids, as the right pterygoid was mirrored from the left and straightened out to create a more accurate depiction of the posterior end of the palate. The basisphenoid is complete and no reconstruction was needed to fit it with the pterygoids anteriorly and the basioccipital posteriorly.

After the reconstruction of the dorsal skull and palate, three incisors were placed back into the premaxilla, depicting how they would have been placed in life. Once reconstruction of the skull of BP/1/7074 was completed, measurements were taken digitally from the reconstruction and then used in an allometric analysis.

### 3.4 Tooth Replacement

Tooth replacement in BP/1/7074 of the canine is clearly visible on the right maxilla of the specimen, as a replacing canine is erupting anteriorly, however replacement of the incisors and postcanines was unknown. Scanning of the specimen allowed for the investigation of the tooth replacement strategies of a juvenile *Anteosaurus* noninvasively.

One replacing incisor was found in the left premaxilla (Figure 3.21). Surprisingly this was the only replacing incisor of the upper jaw found, and suggests that the frequency of replacing canines is much higher than of any other tooth in BP/1/7074. The replacing incisor found in the premaxilla is very small and deep within the alveolus, suggesting that this replacement tooth is at a very early stage of ontogenetic development. This replacing incisor seems to be replacing the fourth incisor on the lingual side, however this is not for certain.

Only one replacement postcanine was found in BP/1/7074 (Figure 3.22). This postcanine is very small, and situated far posteriorly on the left maxilla. Because the new tooth ‘bud’ is positioned deep in the alveolus it is unclear whether or not the replacement tooth is replacing the existing tooth lingually.

Two replacement incisors are present in the left dentary of BP/1/7074 (Figure 3.23 and Figure 3.24). Both of these replacement teeth are replacing the existing

teeth lingually. As is the situation with the incisor in the left premaxilla, both these replacement teeth are underdeveloped and very small.

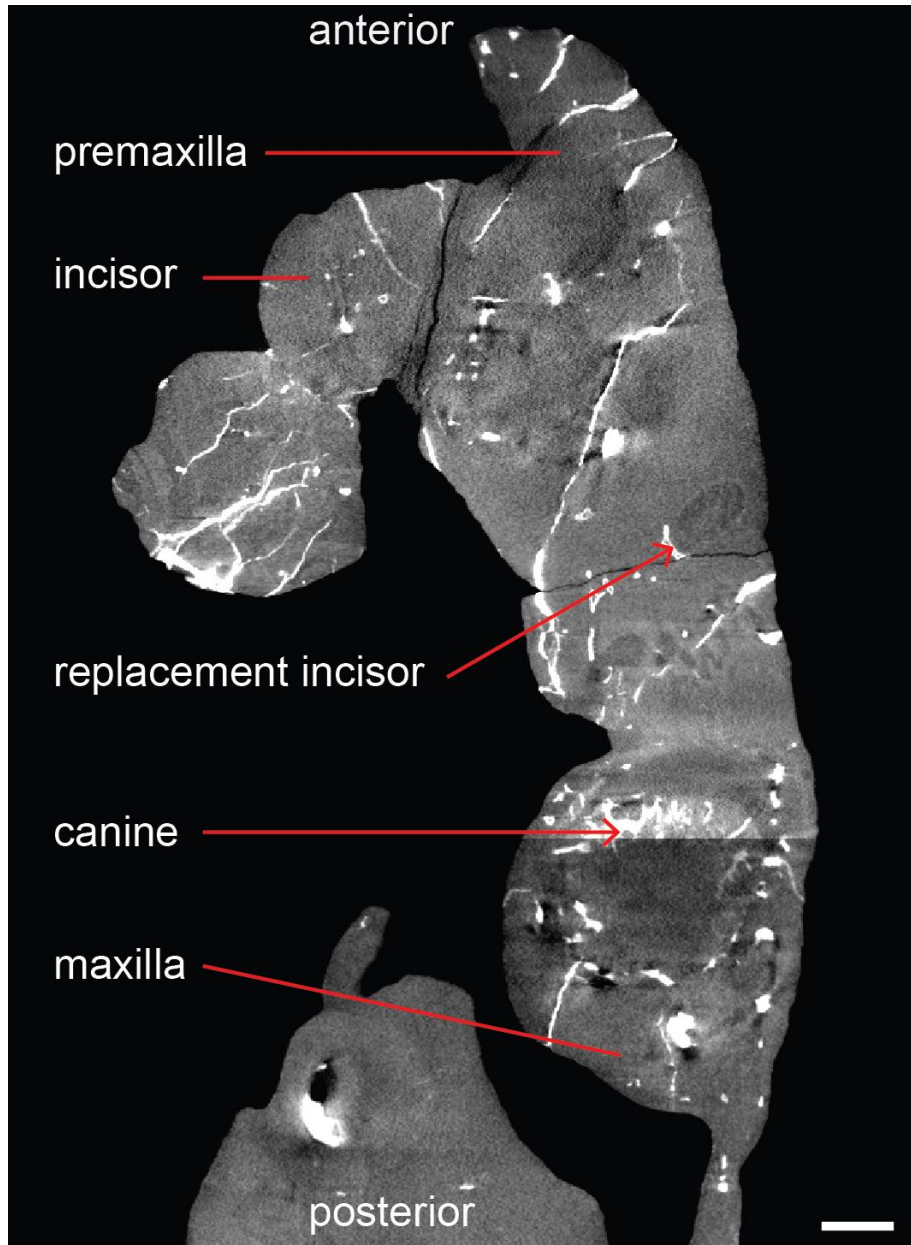


Figure 3.21: C-T slice image of the fourth replacement incisor of the left premaxilla of BP/1/7074. Scale bar equals 1cm.

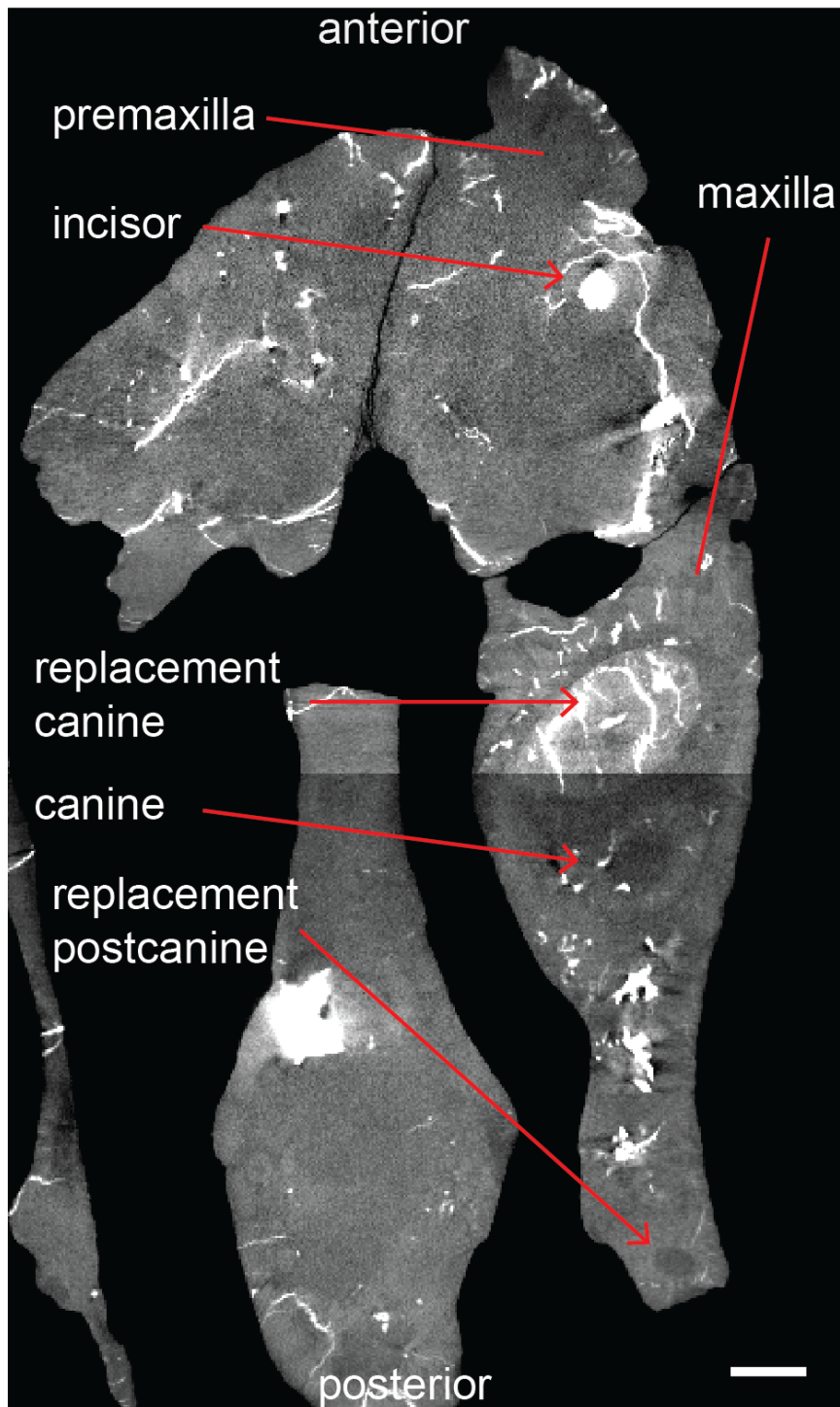


Figure 3.22: C-T slice image of the left maxilla of BP/1/7074 showing the replacement canine and single postcanine. Scale bar equals 1cm.



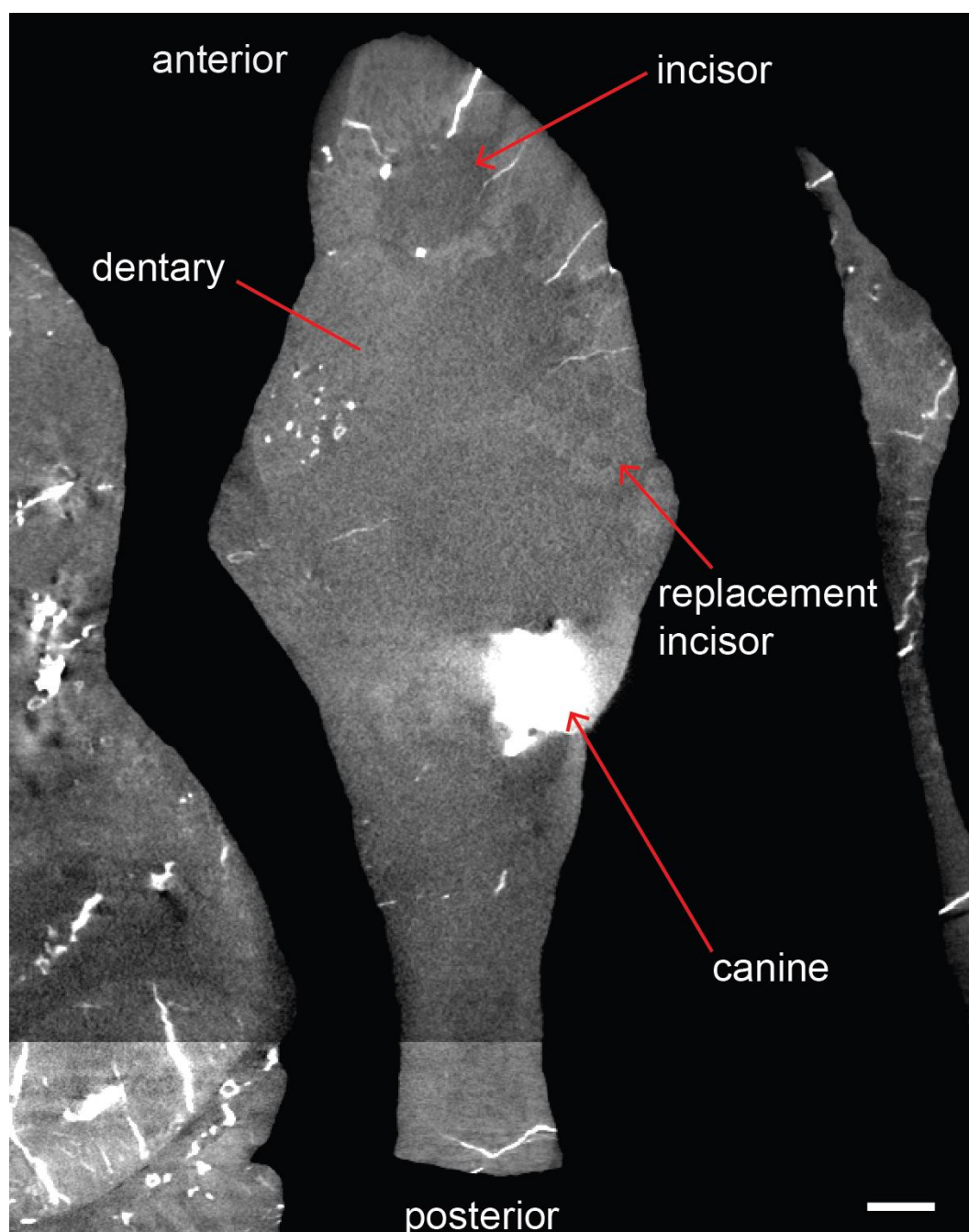


Figure 3.23: C-T slice image of the left dentary of BP/1/7074 showing the fourth replacement incisor. Scale bar equals 1cm.

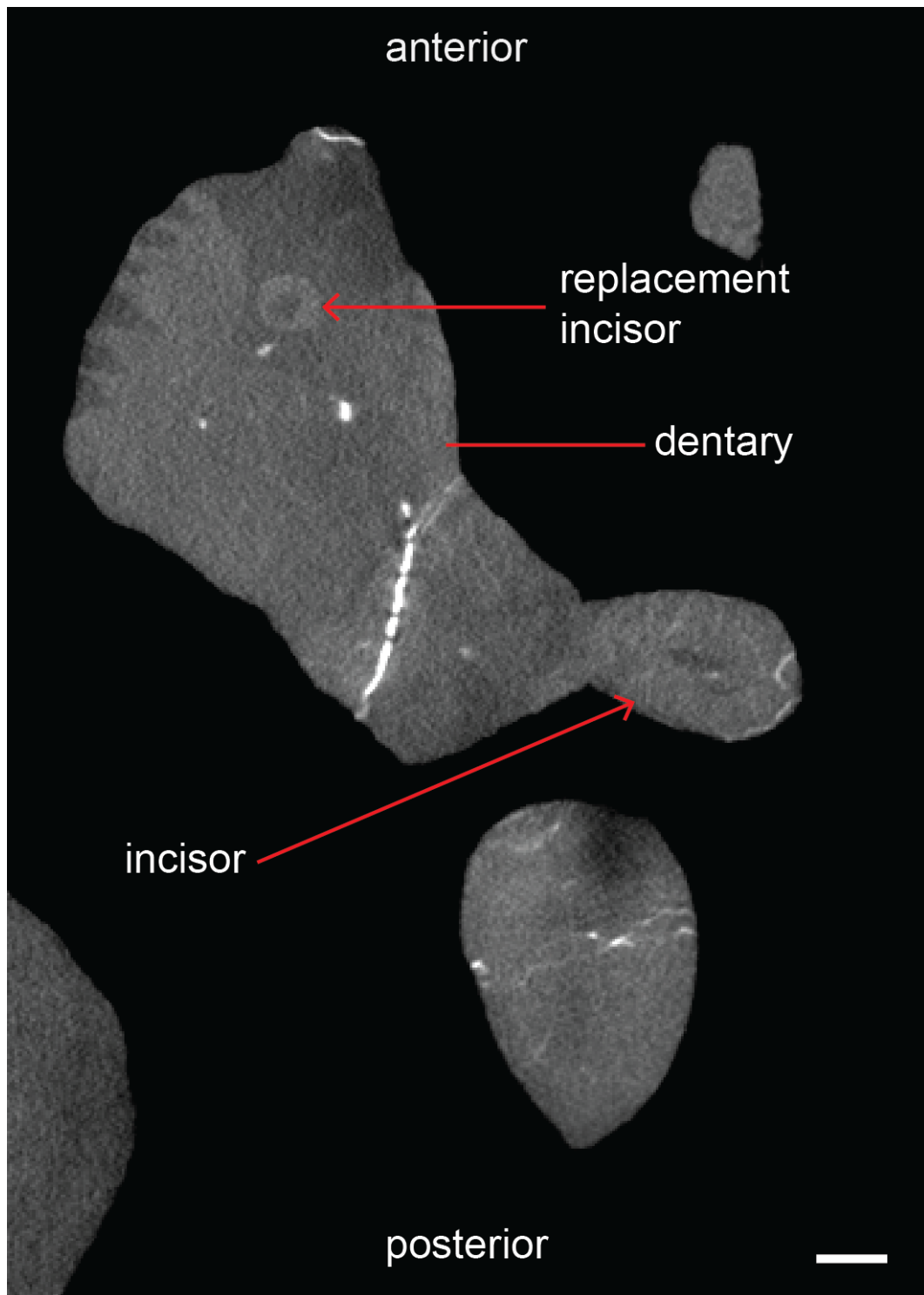


Figure 3.24: C-T slice image of the replacement incisor of left dentary of BP/1/7074. Scale bar equals 1cm.

### 3.5 Allometry

Quantitative allometric analysis was conducted to compare changes of cranial shape along a growth series. The variables analysed in the allometric analysis are presented in Table 3.1. Of the twenty-three variables only four variables have statistical significance with a 95% confidence, indicating that they were different from 1 (isometry). All variables had positive allometry. The four statistically significant variables include: anteroposterior length of temporal fenestra (Variable 7; Figure 3.25); length anterior margin of premaxilla to posterior extremity of posterior process (Variable 13; Figure 3.26); height of jugal below orbit (Variable 21; Figure 3.27); and width of postorbital bar (Variable 22; Figure 3.28).

Considering the reduced sample size because most *Anteosaurus* skulls are incompletely preserved ( $n$  between 6 and 10), it is surprising that allometric growth can be demonstrated. However, despite these constraints allometric growth can be shown for characters that show extreme differences between the smallest and largest specimens of the sample. A discussion of the allometric analysis is presented in Chapter Four.

Table 3.1: Summary of regressions on the length of the skull (tip of snout to parietal foramen) of *Anteosaurus magnificus* (Appendix A: Variable 4).

	Variables	$n$	$R^2$	$\log b_0$	$b_1$	$P (ISO)$
1	Skull width across postorbital bar	9	0.90	-0.52	1.09	0.481
2	Skull width across parietals over pineal opening	8	0.62	-2.39	1.59	0.183
3	Skull width across squamosals	6	0.80	-0.13	1.01	0.964
5	Skull length of tip of snout to anterior margin of orbit	10	0.96	0.04	0.92	0.265
6	Interorbital distance (anterior margin of orbit)	10	0.53	-1.01	1.14	0.608
7	Anteroposterior length of temporal fenestra	8	0.90	-4.34	2.44	0.003
8	Width of temporal fenestra (parietal-postorbital suture in line with pineal foramen to squamosal bar)	6	0.36	-1.85	1.47	0.462
9	Anteroposterior length of postfrontal	8	0.28	-1.39	1.22	0.608
10	Transverse width of postfrontal	7	0.72	-3.03	1.85	0.107
11	Height from lower margin of external naris to alveolar margin immediately behind canine	9	0.72	-2.45	1.64	0.089
12	Distance anterior margin of canine to tip of snout	10	0.75	-1.40	1.29	0.227
13	Length anterior margin of premaxilla to posterior extremity of posterior process	7	0.90	-3.53	2.13	0.0124
14	Anteroposterior width of canine at gumline (largest canine)	9	0.64	-5.32	2.56	0.0717
15	Anteroposterior width of largest second upper incisor at gum line	6	0.01	-4.10	2.05	0.359
16	Anteroposterior length of naris	8	0.48	-3.10	1.77	0.184
17	Dorsoventral height of naris	7	0.22	-0.83	0.88	0.760
18	Distance anterior margin of premaxilla to anterior margin of external nasal opening	8	0.47	-4.02	2.21	0.113
19	Anteroposterior length between anterior margin of parietal foramen and anterior extent of fronto-nasal boss	10	0.26	-3.01	1.99	0.136
20	Transverse distance of canine section	7	0.54	-2.84	1.63	0.257
21	Height of jugal below orbit	9	0.91	-2.37	1.61	0.009
22	Width of postorbital bar	7	0.94	-3.02	1.71	0.011
23	Posterior margin of pineal foramen to occipital rim	6	0.16	-4.32	2.15	0.306

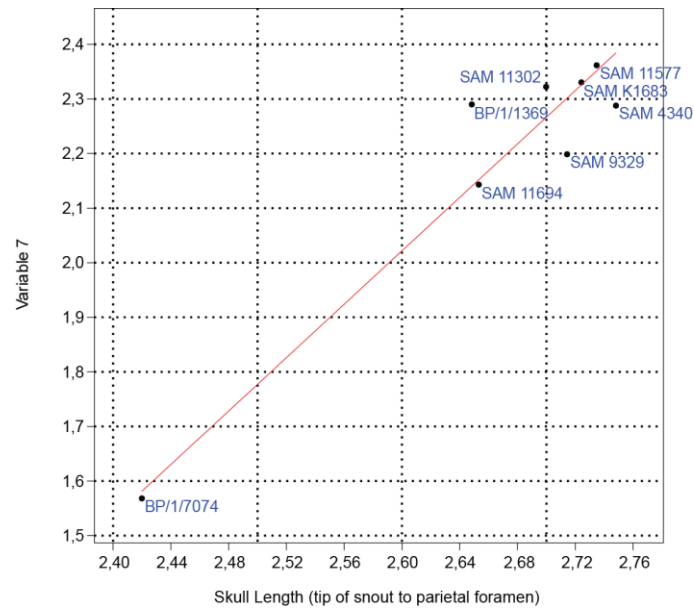


Figure 3.25: Regression of length of the skull (tip of snout to parietal foramen) (log Variable 4) on anteroposterior length of the temporal fenestra (log Variable 7).  $b_1 = 2.44$ .

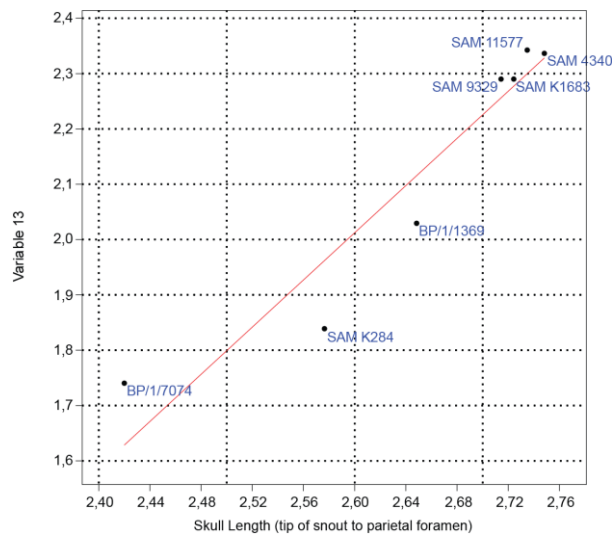


Figure 3.26: Regression of length of the skull (tip of snout to parietal foramen) (log Variable 4) on length of the anterior margin of premaxilla to the posterior extremity of posterior process (log Variable 13).  $b_1 = 2.13$ .

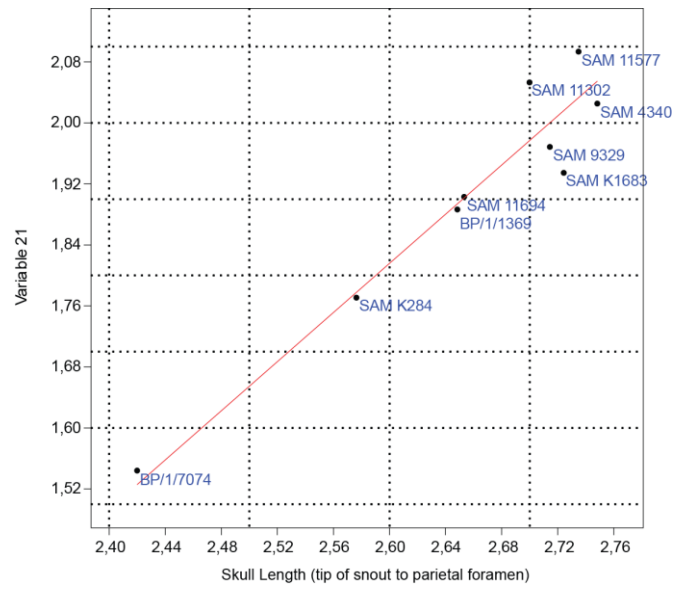


Figure 3.27: Regression of length of the skull (tip of snout to parietal foramen) (log Variable 4) on height of the jugal below the orbit (log Variable 21).  $b_1 = 1.61$ .

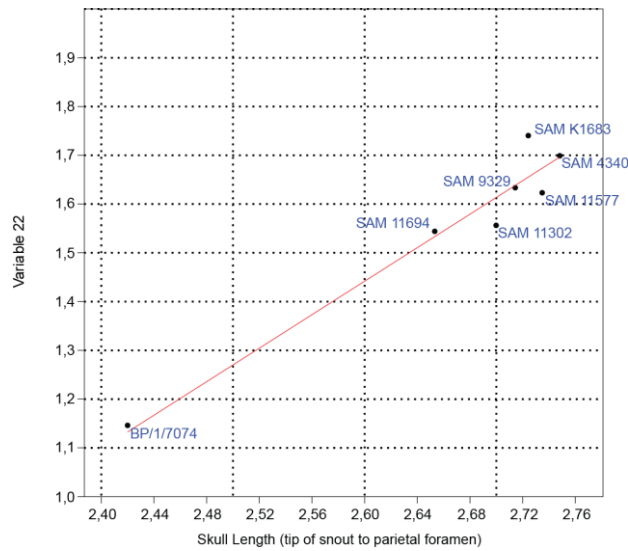


Figure 3.28: Regression of length of the skull (tip of snout to parietal foramen) (log Variable 4) on width of postorbital bar (log Variable 22).  $b_1 = 1.71$ .

## CHAPTER FOUR: DISCUSSION

### 4.1 Growth Model of *Anteosaurus magnificus*

The coefficient suggests that fast growth occurs in the temporal region, indicating the importance of the occlusal musculature in adulthood. Associated with this, the postorbital bar and suborbital bar (height of jugal below the orbit) are strongly positive, suggesting a huge difference in the development of these structures between juveniles and adults. Finally Variable 13 indicates that positive allometry is occurring in the anterior tip of the snout, a trend that is common in several growing amniotes (Emerson and Bramble, 1993).

Additional qualitative trends can be added to the quantitative growth model of *Anteosaurus*. The orbits are proportionally smaller in larger specimens of *Anteosaurus*, a condition that fits in the expected negative allometry for most vertebrates of cranial structure related to the brain and sense organs (Emerson and Bramble, 1993). Many larger *Anteosaurus* specimens show an increase in the angle between the nasal and the frontal of the skull as the skull roof slopes sharply dorsally and the height of the skull increases greatly from the level of the frontal bones, reaching its highest point at the pineal foramen.

In addition to the positive allometry demonstrated for the anterior portion of the snout, the complete snout of BP/1/7074 is shorter in comparison with skull size, than that of large *Anteosaurus* specimens (Figure 4.1). On the positive

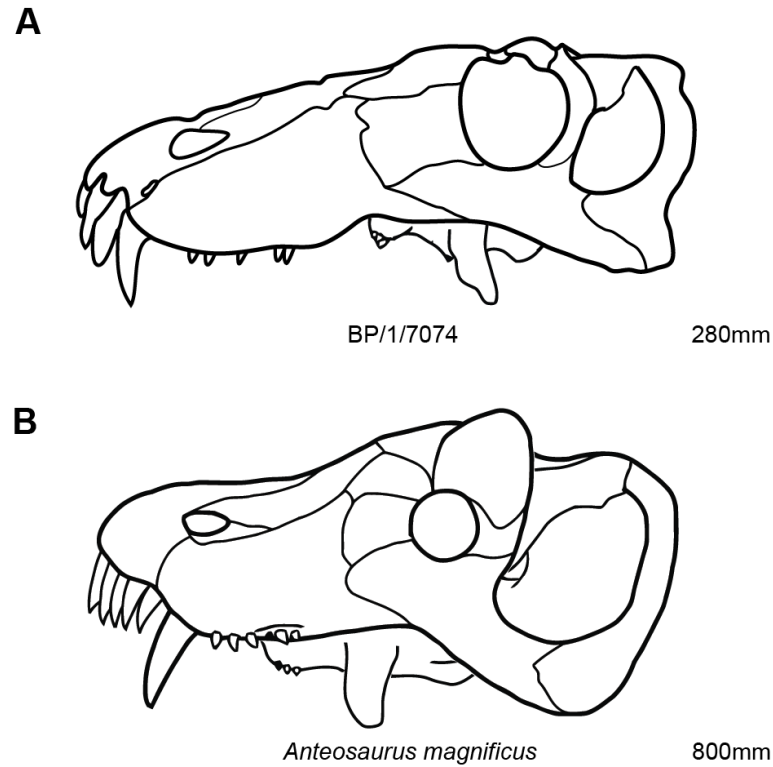


Figure 4.1: Skulls and skull lengths of (A) a juvenile *Anteosaurus magnificus* (BP/1/7074) and (B) an adult *Anteosaurus magnificus* in left lateral view. Skull length is indicated for each specimen in mm. (B after Kammerer, 2011).

allometry of the length of the temporal fenestra it can be added that the temporal fenestra appears proportionally wider in adults, indicating fast growth both in length and width. These changes will result in the occiput being positioned relatively further behind the orbits in larger adult specimens.

A change of sutural relations in the antorbital region between the frontal, lacrimal and jugal is also observed. Both juveniles and adults show an elongated trough between these bones, but this is clearly more prominent in larger specimens.



In the palate, the vomers, palatine and pterygoids are proportionally longer and the pterygoids extends further laterally in largest specimens. In the occiput the pineal foramen, located at the end of a long vertical tube, increases in height and pachyostosis occurs around the pineal boss in larger specimens. Although BP/1/7074 does have a slight pineal boss, the swelling of this boss is much less than that of larger specimens.

Based on the observable differences it can be assumed that many features on the skull roof of *Anteosaurus* change through ontogeny as the angle of the slope of the frontal increases in size with age, the snout increases in length. At the same time the lateral side of the skull projects further laterally at the point of the jugal just below the orbits. In contrast to the situation on the skull roof, in the palate there is only a gradual increase in size occurs relative to age, and there are not many changes in the palatal bones, other than palatal dentition. On the dorsal side the occiput is pushed further back than ventrally and the pineal foramen of large specimens is raised higher above the dorsal skull roof than in the smaller *Anteosaurus* specimen BP/1/7074.

#### **4.2 Heterochronic Process in Anteosauria**

BP/1/7074 has been shown to be *Anteosaurus magnificus* based on having a concave alveolar margin of the precanine region; concave dorsal snout profile; and pachyostosed postfrontals. Because pachyostosis of the frontal has not occurred to the extent of that of the adult specimens, it is much smaller than the

adult specimens, the fact that many of the bones of the skull roof have come apart at the sutures, and its orbits are very large compared to adult forms, BP/1/7074 is considered to be a juvenile. Apart from the canines, which demonstrate tooth replacement in BP/1/7074, only one incisor and one postcanine have any indication of tooth replacement taking place and in both teeth the newly formed tooth 'bud' is still positioned deep in the alveolus. The fact that BP/1/7074 was found very close to an adult *Anteosaurus* specimen (BP/1/7075) and in the exact same stratigraphic horizon, further strengthens the case that BP/1/7074 is a juvenile of *Anteosaurus magnificus*.

It is interesting to compare the skull of the juvenile *Anteosaurus* specimen (BP/1/7074) described in this dissertation with that of different anteosaurid genera. The variation in *Anteosaurus* skull sizes is between 800mm long for the largest specimen (Boonstra, 1954a) and 280mm represented by BP/1/7074. The most striking difference in the ontogenetic sequence of South African *Anteosaurus* is characterised by the strong degree of pachyostosis represented in adults, with development of postfrontal horns and the frontal boss (Kammerer, 2011). There are several features that strongly differentiate the ontogenetic extremes in *Anteosaurus*: orientation of the snout, angulation of the skull roof, height of the skull from the level of the frontal and also the structures which were found to have positive allometry (postorbital bar, suborbital portion of the jugal).

On close comparison with the remaining Anteosaurinae, it is clear that the juvenile morphology of BP/1/7074 is reminiscent of the adult morphology of the

Russian anteosaurid *Syodon biarmicum* (Figure 4.2), with all the above mentioned features that differentiate the juvenile from the adult form of *Anteosaurus*, being similar in the Russian form. This similarity is also the product of the final size of the specimens. The juvenile *Anteosaurus* specimen (BP/1/7074) has a skull length of 280mm similar to that of *Syodon*, described as an adult (PIN 157/2), which is 218mm. The pachyostosis process that plays an important role modifying the skull roof of adult *Anteosaurus* specimens is not present in *Syodon*. Comparison of BP/1/7074 with the small South African basal anteosaurid *Australosyodon* (basal skull length 240mm) shows important differences in the development and orientation of the snout as the snout of *Australosyodon* is much narrower and higher slanting on the dorsal skull.

Results of the tooth replacement assessment has shown that only a few replacement teeth are present. The replacing incisor in the premaxilla is extremely small compared to that of the existing incisor, and is positioned far dorsally within the premaxilla. This is an indication that the replacing incisor is still a 'bud' which was still in development at the time of death. The same is true for the replacing incisors in the dentary, which are positioned far ventrally in the alveolus. These incisors are extremely small compared to the existing incisor in the dentary. Finally the replacing postcanine found in the maxilla is positioned far dorsally in the alveolus, and far posteriorly in the maxilla. The small number of replacing teeth indicates that the specimen had just started to produce replacing teeth at the time of death and was most likely equipped with its first set of incisors and postcanines which had already erupted. However, it is clear that the rate of

replacement of the canines is far higher, as the replacing canine of the right maxilla has already started to erupt. Therefore one can deduce that the canines are the first teeth which are replaced for *Anteosaurus*, followed by the incisors and the postcanines. Furthermore, the lack of fully developed replacing teeth found in BP/1/7074 adds strength to the fact that BP/1/7074 is in fact a juvenile.

Holding Haeckel's Law to be true, the Law states that "evolutionary change occurs by the successive addition of stages to the end of an unaltered, ancestral ontogeny" (Gould, 1977: 74). In the case of the anteosaurids, new characters such as pachyostosis of the skull roof and lateral widening of the suborbital jugal develop following the ontogeny of their ancestors. The juvenile (BP/1/7074) *Anteosaurus* therefore possesses characters similar to that of the more basal genera (*Syodon*) and through its development into an adult, parallels the ontogeny of the most advanced anteosaur descendants (Gould, 1977) to reach a stage that is observed for the adult *Anteosaurus*.

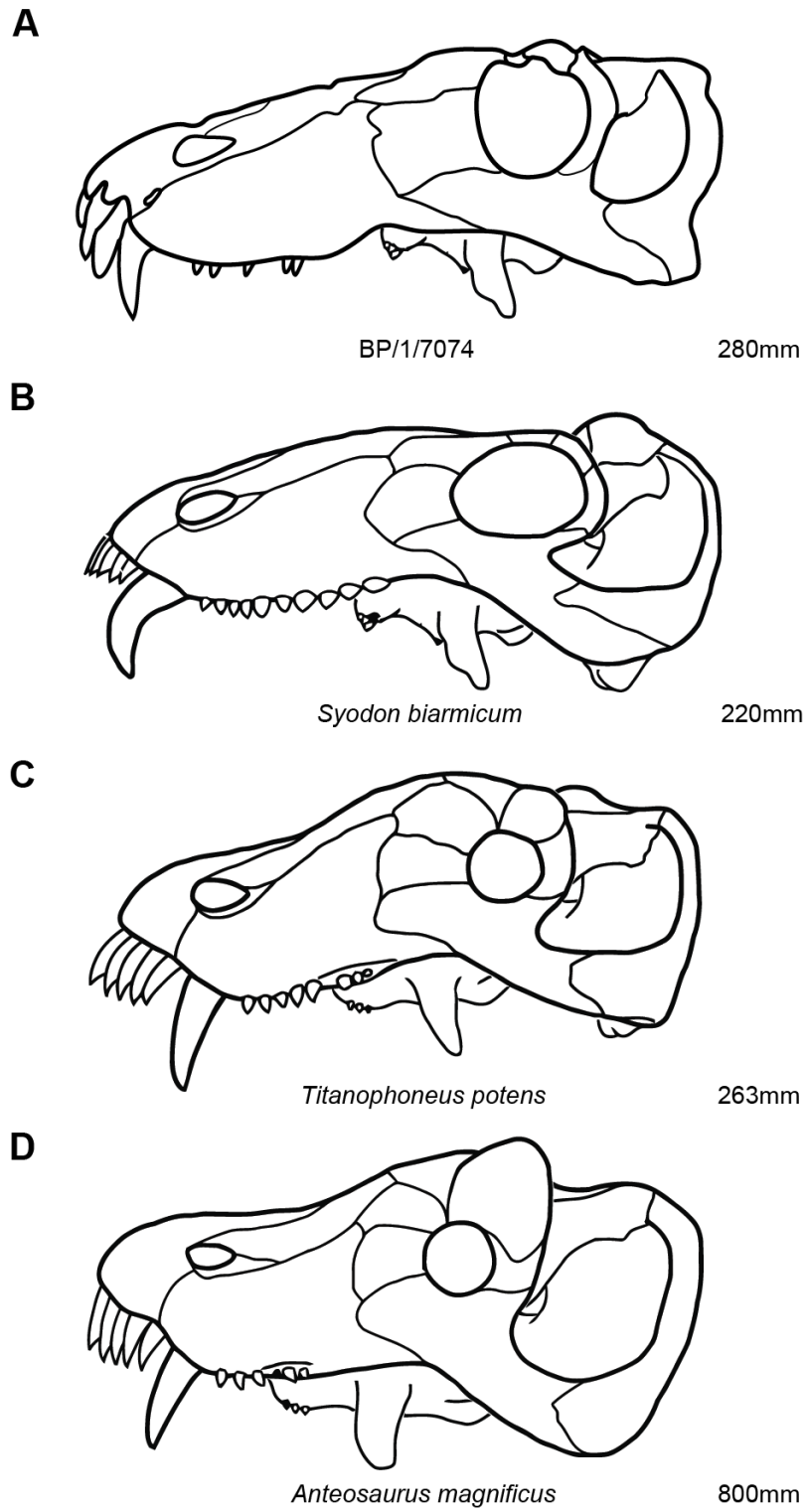


Figure 4.2: Skulls and skull lengths of the anteosaurids (A) juvenile *Anteosaurus magnificus* (BP/1/7074); (B) *Syodon biarmicum*; (C) *Titanophoneus potens*; (D) an adult *Anteosaurus magnificus* in left lateral view. Skull length is indicated for each specimen in mm. (B, C and D after Kammerer, 2011: 292).

### 4.3 Conclusion

The description of BP/1/7074 has shown that it is a juvenile *Anteosaurus magnificus*, based on having a concave alveolar margin of the precanine region and pachyostosed postfrontals. BP/1/7074 has been shown to be a juvenile based on large orbits compared to that of adults, the small size of the skull, bones which have come apart at the sutures, the lack of fully developed replacement teeth, and the superficial morphological resemblance to the more primitive adult Russian anteosaurid *Syodon*. The description presented in this work is the first full description of a juvenile *Anteosaurus* to date. In the process of the description it became clear that the juvenile BP/1/7074 bares remarkable morphological similarities to that of Russian anteosaurids that have been found to be more basal than the South African *Anteosaurus magnificus* (Kammerer, 2011), which is only known from adult specimens thus far. This in turn has led to a definition of the juvenile state of *Anteosaurus*.

The computer-aided 3-D reconstruction included in this work allowed for an accurate rendition of the skull of a juvenile *Anteosaurus* as well as the opportunity to take accurate measurements for an allometric analysis. The reconstruction showed that the specimen (BP/1/7074) was distorted in an anteroposterior direction, and allowed for this distortion to be corrected.

Because of the morphological similarities between the juvenile (BP/1/7074) and basal anteosaurids such as the adult specimen of the Russian *Syodon*, and the

obtained results from the allometric analysis, it is suggested that the ontogenetic growth pattern of *Anteosaurus* follows Haeckel's Law (ontogeny recapitulates phylogeny), in that the juvenile *Anteosaurus* is morphologically very similar to the basal anteosaurid *Syodon*. It has also been shown that the juvenile of *Anteosaurus* (BP/1/7074) lacks some characters which are present in the adult form. Most noticeably these include the extent of pachyostosis of the skull roof which is greatest in the largest skulls. The skull changes shape ontogenetically as the frontal and postfrontals show an increase in pachyostosis, the skull widens laterally at the point of the jugal just below the orbit, and the pterygoids and palatine move more anteriorly in relation to the orbit. At the same time, the pineal foramen shifts dorsally to a position above the skull roof.

This work is the first description of a juvenile *Anteosaurus*. The unfused nature of the cranial sutures, coupled with the lack of replacing incisors and postcanines attest to the early stage of ontogenetic development of skull BP/1/7074. This fact has great potential in determining, for the first time, the ontogenetic development of *Anteosaurus*, as well as to provide input on the phylogenetic development of the *Anteosaurus* skull.

## CHAPTER FIVE: REFERENCES

- Battail, B. and Surkov, M. V. 2000. Mammal-like reptiles from Russia. Pp. 86–119 *In*: Benton, M. J., Shishkin, M. A., Unwin, D. M., Kurochkin, E. N. (Eds) *The Age of Dinosaurs in Russia and Mongolia*. Cambridge University Press, Cambridge.
- Betz, O., Wegst, U., Weide, D., Heethoff, M., Helfen, L., Lee, W., Cloetens, P. 2007. Imaging applications of synchrotron X-ray phase-contrast microtomography in biological morphology and biomaterials science. I. General aspects of the technique and its advantages in the analysis of millimetre-sized arthropod structure. *Journal of Microscopy*, **227**(1): 51–71.
- Boonstra, L. D. 1954a. The cranial structure of the titanosuchian: *Anteosaurus*. *Annals of the South African Museum*, **42**: 108–148.
- Boonstra, L. D. 1954b. The smallest Titanosuchid yet recovered from the Karoo. *Annals of the South African Museum*, **42**: 149–156.
- Boonstra, L. D. 1954c. *Paranteosaurus*, gen. nov.: a Titanosuchian reptile. *Annals of the South African Museum*, **42**: 157–159.



Boonstra, L. D. 1962. The dentition of the Titanosuchid dinocephalians. *Annals of the South African Museum*, **46**: 57–112.

Boonstra, L. D. 1963. Diversity within the South African Dinocephalia. *South African Journal of Science*, **59**: 196–206.

Boonstra, L. D. 1969. The fauna of the *Tapinocephalus* Zone (Beaufort beds of the Karoo). *Annals of the South African Museum*, **56**: 1–73.

Boonstra, L. D. 1971. The early therapsids. *Annals of the South African Museum*, **59**: 17–46.

Boonstra, L. D. 1972. Discard the names Theriodontia and Anomodontia: a new classification of the Therapsida. *Annals of the South African Museum*, **59**: 315–338.

Broom, R. 1910. A comparison of the Permian reptiles of North America with those of South Africa. *Bulletin of the American Museum of Natural History*, **28**: 197–234.

Broom, R. 1929. On the carnivorous mammal-like reptiles of the family Titanosuchidae. *Annals of the Transvaal Museum*, **13**: 9–36.

- Carlson, W. D., Rowe, T., Ketcham, R. A., Colbert, M. W. 2013. Applications of high-resolution X-ray computed tomography in petrology, meteoritics and palaeontology. *Geological Society, London, Special Publications*, **215**: 7–22.
- Cheng, Z. W. and Ji, S. 1996. First record of a primitive anteosaurid dinocephalian from the Upper Permian of Gansu, China. *Vertebrata Palasiatica*, **34**: 123–134.
- Cheng, Z. and Li, J. 1997. A new genus of primitive dinocephalian: the third report on Late Permian Dashankou lower tetrapod fauna. *Vertebrate Palasiatica*, **35**: 35–43.
- Cisneros, J. C., Abdala, F., Atayman-Guven, S., Rubidge, B. S., Celal, Sengor, A. M., Shultz, C. L. 2012. Carnivorous dinocephalian from the Middle Permian of Brazil and tetrapod dispersal in Pangaea. *Proceedings of the National Academy of Science*, **109**(5): 1584–1588.
- Conroy, G. C., and Vannier, M. W. 1984. Noninvasive Three-Dimensional Computer Imaging of Matrix-Filled Fossil Skulls by High-Resolution Computed Tomography. *Science*, **226**(4673): 456–458.
- Crompton, A. W. 1962. On the dentition and tooth replacement in two Bauriamorph reptiles. *Annals of The South African Museum*, **46**: 231–255.

Day, M. O. 2013. *Middle Permian Continental Biodiversity Change as Reflected in the Beaufort Group of South Africa: a Bio- and Lithostratigraphic Review of the Eodicynodon, Tapinocephalus and Pristerognathus Assemblage Zones*. PhD Thesis, University of the Witwatersrand, Johannesburg pp. 387.

DeVore, M. L., Kenrick, P., Pigg, K. B., Ketcham, R. A. 2006. Utility of High Resolution X-Ray Computed Tomography (HRXCT) for Paleobotanical Studies: An Example Using London Clay Fruits and Seeds. *American Journal of Botany*, **93**(12): 1848–1851.

Efremov, I. A. 1940. [Preliminary descriptions of new forms of the Permian and Triassic fauna of terrestrial vertebrates of the USSR: the dinocephalian fauna from the village of Isheevo]. *Trudy Paleontologicheskogo Instituta, Akademiya Nauk SSSR*, **10**: 31–73 [in Russian].

Efremov, I. A. 1954. [The terrestrial vertebrate fauna from the Permian copper sandstones of the western Fore-Urals]. *Trudy Paleontologicheskogo Instituta, Akademiya Nauk SSSR*, **54**: 1–416 [in Russian].

Emerson, S. B. and Bramble, D. M. 1993. Scaling, allometry and skull design. In: Hanken, J. and Hall, B. K. (Eds) *The skull*. University of Chicago Press, Chicago, Illinois. Pp 384–416.

Fernandez, V., Abdala, F., Carlson, K. J., Collins Cook, D., Rubidge, B. S., Yates, A., Tafforeau, P. 2013. Synchrotron Reveals Early Triassic Odd Couple: Injured Amphibian and Aestivating Therapsid Share Burrow. *PLoS One*, **8**(6): 1–7.

Fourie, S. 1974. The cranial morphology of *Thrinaxodon liorhinus* Seeley. *Annals of The South African Museum*, **65**: 337–400.

Gould, S. J. 1977. *Ontogeny and Phylogeny*. Harvard University Press, Cambridge Massachusetts. pp. 501.

Haase, A., Landwehr, G., Umbach, E. (Eds.). 1997. *Röntgen Centennial: X-rays in Natural and Life Sciences*, World Scientific, 708pp.

Hammer, Ø., Harper, D. A. T., Ryan, P. D. 2001. PAST: Paleontological statistics software package for education and data analysis. *Palaeontologia Electronica*, **4**(1): 9pp.

Hancox, P. J., and Rubidge, B. S. 2001. Breakthroughs in the biodiversity, biogeography, biostratigraphy and basin analysis of the Beaufort Group. *African Earth Sciences*, **33**: 563–577.

Haubitz, B., Prokop, M., Dohring, W., Ostrom, J. H., Wellnhofer, P. 1988. Computed Tomography of Archaeopteryx. *Paleobiology*, **14**(2): 206–213.

- Hopson, J. A. 1964. Tooth Replacement in Cynodont, Dicynodont and Therocephalian Reptiles. *Proceedings of the Zoological Society of London*, **142**(4): 625–654.
- Hopson, J. A. and Barghusen, H. R. 1986. An analysis of therapsid relationships. Pp. 83–106 *In*: Hotton, N., MacLean, P. D., Roth, J. J., Roth, E. C. (Eds) *The Ecology and Biology of the Mammal-Like Reptiles*. Smithsonian Institution Press, Washington, D. C.
- Hounsfield, G. N. 1973. Computerized transverse axial scanning (tomography): Part 1. Description of system. *British Journal of Radiology*, 46: 1016–1022.
- Ivachnenko, M. F. 1994. A new Late Permian dromasaurian (Anomodontia) from Eastern Europe. *Paleontological Journal*, **28**: 96–103.
- Ivachnenko, M. F. 1995. Primitive Late Permian dinocephalian-titanosuchids of Eastern Europe. *Paleontological Journal*, **29**: 120–129.
- Ivachnenko, M. F. 2000. *Estemmenosuchus* and primitive Theriodonts from the Late Permian. *Paleontological Journal*, **34**: 189–197.
- Janensch, W. 1959. Eine *Jonkeria* aus der Karru-Formation des Kaplandes. *Paläont. Z.* **33**: 22–49.

- Jirah, S. 2013. *Stratigraphy and Sedimentology of the Middle Permian Abrahamskraal Formation (Tapinocephalus Assemblage Zone) In the Southern Karoo around Merweville, South Africa*. Unpublished MSc Dissertation, University of the Witwatersrand, Johannesburg pp. 132.
- Kammerer, C. F. 2011. Systematics of the Anteosauria (Therapsida: Dinocephalia). *Journal of Systematic Palaeontology*, **9**(2): 261–304.
- Kemp, T. S. 1982. *Mammal-like reptiles and the origin of mammals*. Academic Press, London, pp. 364.
- Kemp, T. S. 2005. *The origin and evolution of mammals*. Oxford University Press, Oxford, pp. 342.
- Kermack, K. A., Tooth replacement in mammal-like reptiles of the suborders Gorgonopsia and Therocephalia. *Philosophical Transactions of the Royal Society, London*, **240**: 95–133.
- Ketcham, R. A., Carlson, W. D. 2001. Acquisition, optimization and interpretation of X-ray computed tomographic imagery: applications to the geosciences. *Computers and Geoscience*, **27**: 381–400.
- King, G. M. 1988. Anomodontia. In: Wellnhofer (Ed.) *Encyclopedia of Paleoherpertology*, 17C. Gustav Fischer Verlag, Stuttgart. pp. 1–174.

- Langer, M. C. 2000. The first record of dinocephalians in South America, Late Permian Rio do Rasto Formation of the Paraná Basin, Brazil. *Neues Jahrbuch für Geologie und Palaontologie, Abhandlungen*. **215**: 69–95.
- Ledley, R. S., Di Chiro, G., Luessenhop, A. J., Twigg, H. L. 1974. Computerized transaxial x-ray tomography of the human body. *Science*, **186**(4160): 207–212.
- Lepper, J., Raath, M. A. and Rubidge, B. S. 2000. A diverse dinocephalian fauna from Zimbabwe. *South African Journal of Science*, **96**: 403–405.
- Li, J. and Cheng, Z. 1995. A new Late Permian vertebrate fauna from the Dashankou, Gansu with comments on Permian and Triassic vertebrate assemblage zones of China. In: Sun, A. I and Wang, Y. Q. (Eds) *Short papers of Sixth Symposium on Mesozoic Terrestrial Ecosystems and Biota*. China Ocean Press, Beijing. pp. 33–37.
- Li, J., Rubidge, B. S. and Cheng, Z. 1996. A primitive anteosaurid dinocephalian from China – implications for the distribution of earliest therapsid faunas. *South African Journal of Science*, **92**: 252–253.
- Liu, J. In press. Osteology, ontogeny and phylogenetic position of *Sinophoneus yumenensis* (Therapsida, Dinocephalia) from the Middle Permian Dashankou Fauna of China. *Journal of Vertebrate Paleontology*.

- Modesto, S.P., Rubidge, B.S., de Klerk, W.J., Welman, J., 2001. A new dinocephalian therapsid fauna on the Ecca–Beaufort contact in the Eastern Cape Province, South Africa. *South African Journal of Science*, **97**: 161–163.
- Nicolas, M., and Rubidge, B. S. 2010. Changes in Permo-Triassic terrestrial tetrapod ecological representation in the Beaufort Group (Karoo Supergroup) of South Africa. *Lethaia*, **43**: 45–59.
- Olson, E. C. 1962. Late Permian terrestrial vertebrates, U.S.A. and U.S.S.R. *Transactions of the American Philosophical Society, New Series*, **52**: 1–224.
- Orlov, J. A. 1958. [Predatory dinocephalians from the Isheevo Fauna (titanosuchians)]. *Trudy Paleontologicheskogo Instituta, Akademiya Nauk SSSR*, **72**: 1–114. [in Russian].
- Owen, R. 1879. Description of fragmentary indications of a huge kind of Theriodont Reptile (*Titanosuchus ferox*, Ow.) from Beaufort West, Gough Tract, Cape of Good Hope. *Quarterly Journal of the Geological Society*, **35**: 189–199.
- Parrington, F. R. 1936. On the Tooth-Replacement in Theriodont Reptiles. *Philosophical Transactions of the Royal Society, London*, **226**: 121–142.



Romer, A. S. 1956. *Osteology of the Reptiles*. The University of Chicago Press, Chicago, 772 pp.

Romer, A. S. 1961. Synapsid evolution and dentition. *In*: International colloquium on the evolution of lower and non-specialized mammals. Brussels, Koninklijke Vlaamse Academic voor Wetenschappen, Letteren en Schone Kunsten van Belgie. Part i: 9-56. Brussels: The Academy.

Romer, A. S. 1966. *Vertebrate Paleontology*. 3rd edition. The University of Chicago Press, Chicago, 468 pp.

Rubidge, B. S. 1991. A new primitive dinocephalian mammal-like reptile from the Permian of southern Africa. *Palaeontology*, **34**: 547–559.

Rubidge, B. S. 1994. *Australosyodon*, the first primitive anteosaurid dinocephalian from the Upper Permian of Gondwana. *Palaeontology*, **37**: 579–594.

Rubidge, B. S. and van den Heever, J. A. 1997. Morphology and systematic position of the dinocephalian *Styracocephalus platyrhynchus*. *Lethaia*, **30**: 157–168.

Schwartz, D., Vontobel, P., Lehmann, E. H., Meyer, C. A., Bongartz, G. 2005. Neutron Tomography of Internal Structures of Vertebrate Remains: A

Comparison with X-Ray Computed Tomography. *Palaeontologia Electronica*, **8**(2) 11pp.

Simon, R. V., Sidor, C. A., Angielczyk, K. D., Smith, R. M. H. 2010. First Record of a Tapinocephalid (Therapsida: Dinocephalia) from the Ruhuhu Formation (Songea Group) of Southern Tanzania. *Journal of Vertebrate Paleontology*, **30**(4): 1289–1293.

Smith, R., Rubidge, B. S., van der Walt, M. 2011. Therapsid biodiversity patterns and paleoenvironments of the Karoo Basin, South Africa. *In*: Chinsamy-Turan, A. (Ed.). *Forerunners of Mammals: Radiation, Histology, Biology*. Indiana University Press.

Sues, H. D. 1986. Locomotion and body form in early therapsids (Dinocephalia, Gorgonopsia, and Therocephalia). Pp. 61–70 *In*: Hotton, N., MacLean, P. D., Roth, J. J., Roth, E. C. (Eds) *The Ecology and Biology of the Mammal-Like Reptiles*. Smithsonian Institution Press, Washington, D. C.

Tchudinov, P. K. 1960. [Upper Permian therapsids of the Ezhovo locality]. *Paleontologicheskii Zhurnal*, **4**: 81–94 [in Russian].

Tchudinov, P. K. 1968. A new dinocephalian from the Cisuralian Region (Reptilia, Therapsida; Upper Permian). *Postilla*, **121**: 1–20.

Tchudinov, P. K. 1983. [Early therapsids]. *Trudy Paleontologicheskogo Instituta, Akademia Nauk*, **202**: 1–227 [in Russian].

Watson, D. M. S. and Romer, A. S. 1956. A classification of therapsid reptiles. *Bulletin of the Museum of Comparative Zoology*, **114**: 35–89.

Watson, D. M. S. 1914. The Deinocephalia, an order of mammallike reptiles. *Proceedings of the Zoological Society of London*, **1914**: 749–786.

Watson, D. M. S. 1921. The bases of classification of the Theriodontia. *Proceedings of the Zoological Society of London*, **1921**: 35–98.

## APPENDIX A

List of measurements taken for allometric analysis:

1. Skull width across postorbital bar
2. Skull width across parietals over pineal opening
3. Skull width across squamosals
4. Skull length tip of snout to middle of parietal foramen
5. Skull length of tip of snout to anterior margin of orbit
6. Interorbital distance (anterior margin of orbit)
7. Anteroposterior length of temporal fenestra
8. Width of temporal fenestra (parietal-postorbital suture in line with pineal foramen to squamosal bar)
9. Anteroposterior length of postfrontal
10. Transverse width of postfrontal
11. Height from lower margin of external naris to alveolar margin immediately behind canine
12. Distance anterior margin of canine to tip of snout
13. Length anterior margin of premaxilla to posterior extremity of posterior process
14. Anteroposterior width of canine at gumline (largest canine)
15. Anteroposterior width of largest second upper incisor at gum line
16. Anteroposterior length of naris
17. Dorsoventral height of naris

18. Distance anterior margin of premaxilla to anterior margin of external nasal opening
19. Anteroposterior length between anterior margin of parietal foramen and anterior extent of fronto-nasal boss
20. Transverse distance of canine section
21. Height of jugal below orbit
22. Width of postorbital bar
23. Posterior margin of pineal foramen to occipital rim

## Appendix B

Table of distances (in mm) of the different measurements presented in Appendix A for the ten most completely preserved skulls of *Anteosaurus magnificus*:

	1	2	3	4	5	6	7	8	9	10	11	12	13	14	15	16	17	18	19	20	21	22	23
<b>SAM K284</b>	210	41		377	244	88			35	34	55	77	69				45	21	82	27	59		
<b>BP/1/1369</b>	220			445	328	136	195	182			51	77	107	90	61	20			84	15	77		
<b>SAM 11577</b>	310	90	520	543	375	124	230	179	93	120	114	156	220	35		68	45	89	273	35	124	42	43
<b>SAM 4340</b>	278		392	560	395	88	194		81	105	119	156	217	37	25	58	38	114	263		106	50	
<b>SAM K1683</b>	286	80	400	530	375	125	214	113	85	105	110	139	195	26	13	55	31	99	270		86	55	28
<b>SAM 9329</b>	266	102	342	518	356	126	158	85	95	100	89	125	195	35	16	51	30	107	245		93	43	15
<b>SAM 11302</b>		86		501	337	158	210				122	110		32		59	30	94	260		113	36	
<b>SAM 11492</b>	226	70		371	273	86			64	82		93		30	13				204	19			47
<b>SAM 11694</b>	220	44	360	450	315	109	139	113	65		83	104		31		40		79	237	25	80	35	15
<b>BP/1/7074</b>	125	37	215	263	200	65	37	66	68	37	45	67	55	8?	17	26	12	49	156	70	35	14	11